THERMAL ENERGY STORAGE

Systems and Applications

İbrahim Dinçer
KFUPM, Dhahran, Saudi Arabia
and
Marc A. Rosen
Ryerson Polytechnic University, Toronto, Canada

with contributions from

A. Bejan
Duke University, USA

A. J. Ghajar
Oklahoma State University, USA

K. A. R. Ismail
FEM-UNICAMP, Brazil

M. Lacroix
Université de Sherbrooke, Canada

Y. H. Zurigat
Sultan Qaboos University, Oman

JOHN WILEY & SONS, LTD

6

Heat Transfer and Stratification in Sensible Heat Storage Systems

Y.H. Zurigat and A.J. Ghajar

6.1 Introduction

The importance of Thermal Energy Storage (TES) as an energy conservation and management tool has been discussed in previous chapters. In this chapter we focus on the problem of sensible heat storage in liquids for low-to-medium temperature ranges and the associated developments to date. The choice of the type of liquid for sensible TES depends on its specific heat, mass density, toxicity, corrosion resistivity, and cost, and on the operating temperature range. The volumetric heat capacity, ρC_p, defined as the heat storage per unit volume and unit temperature difference, determines the volume of the storage device, while the working pressure of the storage system determines the operating temperature range. High storage temperatures require low-vapor-pressure liquids or pressurized tanks. Both options are often costly to implement (Wyman *et al.*, 1980). Water, due to its abundance, low cost, high specific heat and benign characteristics, is the most widely used storage medium in the low-to-medium thermal-storage temperature range. This temperature range covers chilled water storage at about 4°C and hot water storage below 100°C. Also, since water is the working fluid in many energy systems, its choice as a thermal storage medium is natural. Hot and chilled water storage can be easily integrated with existing building heating and cooling systems. This way, the use of heat exchangers is eliminated, thereby avoiding the extra cost of heat exchangers and the thermal losses associated with their use. The practical problems associated with using water are the possibility of freezing in cold weather and the corrosion of steel storage vessels and piping. Circumventing these problems is relatively straightforward, i.e. insulating the storage device or locating it indoors or underground at a safe depth and using corrosion inhibitors and other corrosion protection measures. Therefore, in this chapter we focus on sensible heat storage in water and the associated heat transfer phenomena. This involves both hot and cold storages in practical applications, e.g. air conditioning, solar energy technologies, heat pumps, gas turbines, and other energy systems.

In the majority of solar energy collection systems water is heated during the day and stored for use during the night, thus extending the use of solar energy over a larger part of the day. Chilled water, on the other hand, is used for cooling in the air conditioning systems in buildings and in gas turbine power plants to cool the inlet air. Chilled water storage can shift part of the cooling requirements to off-peak hours, resulting in improved utility load factors, in addition to allowing the chillers to operate during the cooler night temperatures, resulting in improved coefficients of performance. The economical impact extends beyond this to the owners who not only avoid the extra demand charges during peak demand periods, but also take advantage of discounted night-time rates. Moreover, since the equipment does not have to handle the peak load its size is minimized, resulting in savings in capital investment. That is, instead of installing two chillers to operate at full load during the peak hours and at partial load during the rest of the demand period, one may install a smaller single chiller operating 24 hours per day to charge the storage tank during off-demand periods. The tank in turn assists the chiller during the demand period. Some gas-turbine power plants utilize chilled water to cool inlet air in order to boost the power output during the hot season. That is, at night when the demand is low and the air is cool, water is chilled and stored for use during the daytime peak demand period. This way the gas turbine operates longer at its high efficiency level, and the need for additional equipment to handle the peak demand is minimized.

Hot or chilled water is stored in tanks, which vary in design as dictated by different factors, like thermal performance, and architectural, retrofit and economical constraints. However, all existing thermal storage tank systems share the same objective of maintaining the thermodynamic availability of stored energy so that it can be extracted at the same temperature at which it was stored.

The separation of any fluids at different temperatures in storage tanks is the key factor in achieving this objective. The *two-tank* system (also called the *empty tank* design) is one obvious way of achieving the separation. In this system two identical tanks are used: the first tank is in the charge mode to store the heated or chilled water; and the second tank is used to store the discharged water as it exits the load. Once the stored water is fully discharged the first storage tank becomes empty and ready to be charged with water from the second tank via the heat source or the chiller. Although this design ensures separation of hot and cold water, it is not the best choice with regard to simplicity, economic feasibility, and space utilization. Other schemes have been designed and implemented. These include a single tank with a *flexible diaphragm* mounted either horizontally or vertically, *labyrinth tanks* in which the water is forced to flow through a maze, and the single *stratified tank* in which use is made of the natural process of stratification that permits the hot water to float on top of the cold water. The single tank with a flexible diaphragm has been used in several installations. Although the diaphragm prevents blending of hot and cold water, concerns about membrane maintenance, durability and cost have been raised (Tamblyn, 1980). The *labyrinth tanks* concept was developed in Japan, where many buildings have earthquake protection structures under the basement floor in the form of intersecting high-tie beams.

With little modification the resulting space compartments can be used to store chilled or hot water, and they are connected in such a way to force the water in a plug flow with minimal mixing between the hot and cold regions. A model tank employing this concept was tested by Tamblyn (1980), and on a single-pass test it proved to be efficient in

separating the hot and cold liquid water, but its performance was found to deteriorate in cyclic tests. Of course, unless the suitable structure is available for no extra cost as in Japan, the economics of this concept is unlikely to compete with equally efficient anti-blending systems.

Because of the modest temperature ranges involved, the storage of significant amounts of thermal energy involves relatively large tanks, which must therefore be simple and cheap in construction in order to be economically viable. Also, to apply this technology to residential use, the operation of the tanks must be simple, reliable, and low in maintenance; it cannot involve elaborate monitoring, valving, and control systems. The last concept in the list, the single *stratified tank* (see Figure 6.1), satisfies these requirements, and thus is the most attractive choice in low-to-medium temperature thermal-storage applications due to its simplicity and low cost. Furthermore, the research and development efforts have led to performance comparable with the other storage types employing physical barriers (Tran *et al.*, 1989). Stratified tanks as large as 4 million gallons (15,140 m^3) have been installed in the US for chilled water storage. In the US chilled water storage constitutes about 34% of the cooling capacity of all cool storage systems. 60% of chilled water storage systems utilize stratified tanks (Musser and Bahnfleth, 1998). Clearly, stratified thermal storage has become an essential element in load management and energy conservation technology.

In this chapter the experimental and modeling efforts and the resulting advances in the technology of stratified thermal storage in water are presented. The next section introduces the flow and heat transfer phenomena followed by the performance measures and experimental and theoretical foundations. One- and two-dimensional models of flow and heat transfer are then discussed. We then conclude with a summary on design recommendations.

6.2 Fluid Flow and Heat Transfer Aspects

The principle of operation of stratified thermal storage tanks is based on the natural process of stratification, and hence the fluid flow within these tanks involves both forced and natural convection. In heat storage applications the cold fluid withdrawn from the bottom of the tank is heated at the heat source, i.e. solar collector, heat pump, or gas-fired or electric resistance heaters, and is returned to the top of the tank at relatively higher temperature (see Figure 6.1). Assume for now that the temperature of the incoming stream remains constant at its elevated value. The incoming flow possessing momentum will tend to mix with the fluid in the tank. However, being at a higher temperature, the resulting buoyancy tends to lift the stream restricting its motion to the surface region. This way mixing is restricted to a limited region at the surface near the inlet. As more fluid is introduced, the fluid in the mixing region is pushed down, leaving behind a region of uniform temperature equal to the inlet temperature. The region of intermediate temperatures separating this uniform temperature region from that initially in the tank is termed a *thermocline*. It is defined as the region of steepest temperature gradient separating the hot and cold fluid regions in the tank. The buoyancy arising from the stable density gradient across the thermocline region inhibits mixing between the hot and cold fluid regions on either side. Thus, the thermocline acts as a physical barrier. The thickness of the thermocline region is an important indicator of how well the stratified tank is designed.

This thickness is a function of several variables: the geometry of the tank and the inlet(s), and the hydrodynamic and thermal characteristics of the flow in the tank. The way the flow is introduced and the balance between buoyancy and inertia forces are detrimental to the formation of a thin thermocline. Once the thermocline is formed it travels down as the charging continues until it exits the tank, indicating full charge.

In the discharge mode the load flow loop is activated and the process described above is reversed. That is, the hot water is withdrawn from the top and is replaced by cold water introduced from the bottom. This could be the discharged water cooled at the thermal load or the makeup water in the case of hot water consumption. The flow momentum tends to blend the incoming fluid with the fluid in the tank while the buoyancy now acting downward tends to make the incoming stream flow in a gravity-current form below the relatively warmer fluid. A thermocline is formed and it travels up the tank separating the cold and hot fluid regions. A portion of the thermocline may exit the tank depending on the allowable temperature at the load. Frequently, a load flow loop may operate simultaneously alongside the charging loop. In this case, the tank may experience a net charge or discharge depending on the relative magnitudes of the flow rates of the corresponding loops.

The same phenomenon occurs in chilled water storage tanks, but the charge and discharge flow directions are reversed. One major difference, however, exists. That is, the operating temperature is relatively low, and consequently the density differences are very small (see Figure 6.2) and the stratification is weak, leading to a tendency for chilled water to mix excessively with warmer water in the tank, if disturbed by uncontrolled inlet flows.

In the foregoing discussion it is assumed that the inlet temperature remains constant. In solar collector systems this condition is never satisfied unless some measures are used to control the flow rate through the collector. In reality, water heated by solar panels varies continuously in temperature, resulting in buoyant flows which seek equilibrium with the fluid in the tank. This enhances mixing in the tank, and the thermocline region defined earlier is no longer clearly visible. That is why the term thermocline is reserved for the constant inlet temperature condition. To avoid excessive mixing the flow must be inserted into the stratified thermal storage tank at the proper level with minimum mixing on the way. This was the object of several designs that remove the momentum of the inlet stream while allowing it to distribute itself to the proper stratification level (see section 6.4).

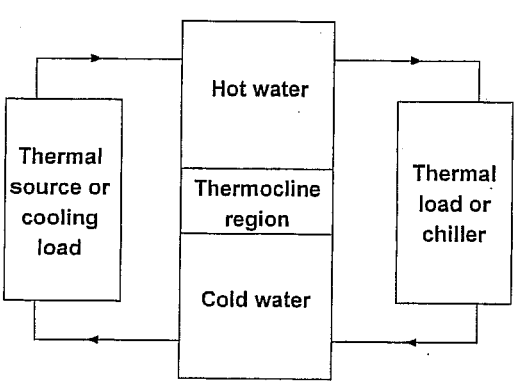

Figure 6.1 Single stratified thermal storage tank integrated with heating or cooling systems.

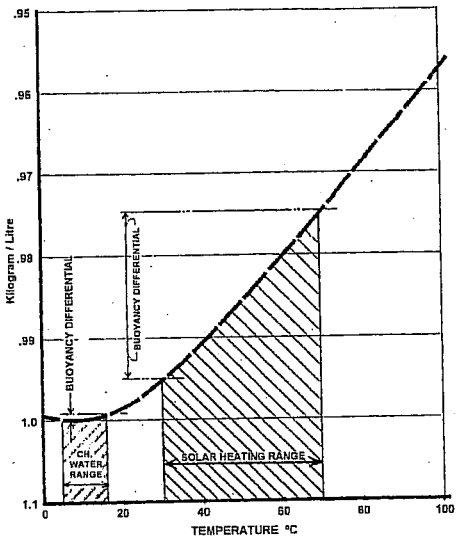

Figure 6.2 Buoyancy differentials typical of solar heating and chilled water applications (Tamblyn, 1980).

Maintaining stratification in storage tanks is essential for better performance of energy systems with which these tanks are integrated. Solar collectors operate at higher efficiency as the collector inlet temperature is decreased (Duffie and Beckman, 1980). Stratification improves the overall performance of solar collector systems by reducing the average absorber plate operating temperature. Performance improvements reported in the literature are 10% (Davis and Bartera, 1975), 5–15% (Sharp and Loehrke, 1979), and 5–20% (Cole and Bellinger, 1982). Simulations with ideally stratified and fully mixed storage tank models show improvements in annual collector system performance ranging from 11.5–18.5% when using the ideally stratified model (Wuestling *et al.*, 1985). Improvements as high as 37% were also reported by Hollands and Lightstone (1989). If a thin thermocline is maintained in chilled water storage tanks the water delivered to the cooling system is at the lower temperature for most of the discharge period. This way, smaller flow rates and pumping power are needed to satisfy the cooling requirements as opposed to the case of a chilled water tank with a high degree of mixing. As a result, maintaining stratification was the object of many research works, both experimental and analytical. These will be discussed in the following sections.

The loss of stratification in liquid thermal storage tanks is associated with several factors that manifest themselves in two ways: the mixing introduced by the inlet streams during charge or discharge; and the heat transfer that may take different paths. In thermocline TES tanks (constant inlet temperature), the mixing during the formation of thermocline at the inlet for the charge and the discharge is the major contributor to the loss of thermodynamic availability of stored energy. This mixing remains difficult to evaluate as it depends on the type of inlet and the flow conditions. A discussion of the modeling efforts of this process is introduced later. In static and dynamic modes of operation of stratified thermal storage tanks, three non-mixing heat transfer paths are present. Nonetheless, they may lead to convective currents and subsequent mixing. These are the

heat transfer to the ambient surroundings through the tank envelope and insulation, heat diffusion in the water body through the thermocline, and heat leakage from the high temperature to the low temperature regions by means of axial conduction through the wall. These heat transfer processes may seriously affect thermal stratification and lead to its degradation. The governing parameters in these are the temperature difference between the hot and cold regions of stored fluid, the wall thermal conductivity, the wall thickness, the insulation type, the size of the tank, and the temperature of the ambient surroundings. It should be noted that some experimental works were successful in isolating the effect of a particular path, while others studied the combined effect of the three heat transfer paths.

In the analyses of stratified tank problems, several dimensionless numbers arise. Noting that the flow in the thermal storage tank is of the mixed convection type, the relative magnitudes of the buoyancy and inertia forces play a major role in the flow development. This was expressed in what is known as the dimensionless Richardson (also called Archimedian) number as $Ri = Ar = Gr / Re^2 = g\beta\Delta T\ell_r / u_r^2$, where the subscript r denotes a reference quantity, Gr is the Grashof number arising in free convection flows and Re is the Reynolds number. Also, the Peclet number, Pe, is used to characterize the relative magnitudes of the thermal energy transported by fluid motion to that transported by molecular diffusion. In terms of other numbers, $Pe = RePr$, where Pr is the Prandtl number. These numbers are often written with a subscript showing the reference length scale. For example, Re_D and Pe_H mean that the Reynolds number is based on the diameter and the Peclet number is based on the height. Frequently, the Froude number, Fr, is used, which is equal to the square root of the ratio of the inertia and gravity forces, $Fr = u_r / \sqrt{g\ell_r}$. A modified Froude number, Fr_m, is also used which is based on the buoyant force per unit mass, $g\beta\Delta T$, instead of the gravitational force per unit mass, g. That is, $Fr_m = u_r / \sqrt{g\beta\Delta T\ell_r}$. The square of the modified Froude number may be expressed in terms of the numbers already defined, i.e. $Fr_m^2 = 1/Ri = u_r^2 / g\beta\Delta T\ell_r$. Sometimes, the temperature difference in Ri and Fr_m is expressed in terms of the density difference as $\beta\Delta T = (\rho_r - \rho)/\rho_r$, where ρ_r is the reference density. Using this substitution in the modified Froude or Richardson numbers, we then talk of the densimetric modified Froude, Fr_{dm}, and densimetric Richardson, Ri_d, numbers. The reference quantities used in these numbers need to be ascertained when interpreting the results in the literature. This is because different investigators use different reference quantities. For example, the Reynolds and Richardson numbers used by Cabelli (1977) were based on the inlet port velocity and the height of the tank. Lavan and Thompson (1977) based the Grashof number on the diameter of the tank and the Reynolds number on the inlet port diameter. As a result, for the same test conditions a number quoted by one investigator may be quoted by another as being of several times the order of magnitude.

6.3 Performance Measures

Typically, the experimental and computational results of stratified thermal energy storage presented in the literature consist of transient temperature profiles under different thermal,

hydrodynamic, and geometric conditions. To quantify the effects of these conditions on thermal stratification, different performance measures have been devised, depending on the conditions under consideration. For example, in thermocline TES tanks of the same geometry the effects of different flow conditions and inlet configurations may be judged based on the *thermocline thickness* they produce. Although a thicker thermocline is associated with a larger degradation of stored energy, the thermocline thickness does not give a quantitative measure of how large this degradation is. Also, this measure cannot be used in the variable inlet temperature condition in which a well-defined thermocline is not present. Furthermore, the thermocline thickness cannot be used for judging competing designs of different geometries. Thus, some other measures have to be used. In this section we look at different measures of performance used by different investigators. This material should help in the proper interpretation of the results cited in this chapter.

In many instances the effect of different parameters on stratification is judged in reference to the temperature profiles predicted by theoretical models such as the ideal model of plug flow, the fully stratified model, or the fully mixed flow model. These are discussed in section 6.5. The relative performance of different designs is then gauged by the departure of their corresponding test results from those predicted by these models. This is a very common approach used by many investigators because it gives quick visual comparisons. Abu-Hamdan *et al.* (1992) used this technique to compare the performance of three different inlet configurations under variable inlet temperature conditions. They calculated the instantaneous thermal efficiency of a simulated solar collector fed by water from the bottom of storage tank at three different outlet temperature profiles. These were the measured profile and those calculated for the same tank from the fully mixed and the fully stratified models. Also, the *mix number* of Davidson *et al.* (1994), discussed later in this section, is based solely on the above-mentioned technique.

One of the other measures was the *degree of stratification* used by Sliwinski *et al.* (1978), and it is characterized by the temperature gradient $\Delta T/\Delta X$ in the thermocline region. Once the thermocline is formed this gradient was calculated at any time by locating points on the temperature profile such that the gradient was less than the maximum gradient for that profile by 10%. For each experiment a mean gradient was calculated by averaging the gradients so calculated. Then the mean gradient is non-dimensionalized by the initial overall temperature gradient defined by $\Delta T_o/H$, where $\Delta T_o = (T_h - T_l)$, where T_h and T_l are the initial high and low temperatures, respectively, and H is the distance between the inlet and the outlet. This ratio was later called the *stratification number*, and was used by other investigators (e.g. Al-Najem, 1993) to quantify the rate of decay of thermal stratification in the static mode of operation.

The *extraction efficiency* is another performance indicator used in the dynamic mode of operation. It was first defined for the discharge of hot water storage tanks as

$$\eta = \frac{\dot{\forall} t_d}{\forall_T} \tag{6.1}$$

where $\dot{\forall}$ and $\forall_T$ are the volumetric flow rate and the internal volume of the tank, respectively, and t_d is the discharge time required for the outlet-to-inlet temperature difference to drop to a pre-assigned percentage of its value at the start of the discharge. Lavan and Thompson (1977) used a 10% drop, i.e. $(T_e(t) - T_{in})/(T_o - T_{in}) = 0.9$. The

extraction efficiency so defined represents the useful fraction of the initially stored volume. Therefore, it does not quantify the recovered fraction of stored heating or cooling capacities. The extraction efficiency may also be interpreted as the dimensionless discharge time, $t^* = \dot{\forall}\, t_d / \forall_T$, that has a value of unity for tanks with the ideal plug flow and less than unity for actual tanks. That is, in the plug flow case with no thermal losses of any kind the thermocline thickness is zero, and all the tank volume will be extracted during the discharge. The extraction efficiency in terms of the tank height, H, and the mean vertical velocity in the tank, V, is $\eta = t^* = V t_d / H$. In addition to the above expression for the extraction efficiency, Ismail *et al.* (1997) used the ratio of the integrated heat discharged over that which results from a plug flow with zero thermocline thickness. That is,

$$\eta = \frac{1}{\Delta T_o} \int_0^1 \left(T_e(t) - T_\ell\right) dt^* \tag{6.2}$$

The integration time limit is that at which one tank volume is discharged. The extraction efficiency defined by Equations 6.1 and 6.2 were both used by Ismail *et al.* (1997), and negligible difference in the results was observed. This is, of course, typical of thermocline thermal storage in the discharge mode, where the temperature profile experiences a sharp drop towards the low-temperature value resulting in the small difference found.

To evaluate the effects of stratification degradation mechanisms in a static hot water storage tank, Abdoly and Rapp (1982) used the *fraction of recoverable heat, F(t)*, as a measure of the heating capacity of an initially charged tank at temperature T_h. *F(t)* was defined as the ratio of the heating capacity available at any time, $Q(t)$, to that initially stored, Q_o. Thus,

$$F(t) = Q(t)/Q_o \tag{6.3}$$

The recoverable heat $Q(t)$ is calculated based on an arbitrarily set criterion. That is, the tank is subdivided into a number of small uniform temperature regions, and the heat stored in any fluid region is considered useless, i.e. $Q(t) = 0$, if its temperature drops below a specified useful temperature dictated by the load requirements. Abdoly and Rapp (1982) considered the heat of any fluid element, J, useful if its temperature, T_J, did not drop below its high initial value, T_h, by more than 20% of the initial high-to-low temperature difference, i.e. $T_J \geq T_\ell + 0.8(T_h - T_\ell)$. Thus, the heat recovered from a fluid region J of mass m_J and temperature T_J is:

$$Q_J(t) = \begin{cases} 0 & \text{if } (T_J - T_\ell)/(T_h - T_\ell) < 0.8 \\ m_J C_p (T_J - T_\ell) & \text{if } (T_J - T_\ell)/(T_h - T_\ell) \geq 0.8 \end{cases} \tag{6.4}$$

The total heat recoverable, $Q(t)$ from the tank with total water mass, M_T, is found by integrating over all fluid elements, i.e.

$$Q(t) = \Sigma Q(t)_J \tag{6.5}$$

and

$$Q_o = M_T C_p \left(T_h - T_\ell\right) \tag{6.6}$$

Murthy *et al.* (1992) used the above method for assessing the effect of wall thermal conductance on stratification in model storage tanks. The advantage of this method is its simplicity. Also, it is an accurate measure of comparative performance. Nelson *et al.* (1999) applied the same method for evaluating the performance of chilled water storage. They defined Percent Cold Recoverable (PCR), instead. The useful temperature considered by Nelson *et al.* (1999) was that which does not rise above the low (cold) water charging temperature, T_ℓ, by more than 20% of the initial temperature difference. That is, $T_J \le T_\ell + 0.2(T_h - T_\ell)$. The PCR is calculated from Equation 6.3 with Equations 6.5 and 6.6 as before, and Equation 6.4 is rewritten as

$$Q(t)_J = \begin{cases} 0 & \text{if } (T_J - T_\ell)/(T_h - T_\ell) > 0.2 \\ m_J C_p (T_h - T_J) & \text{if } (T_J - T_\ell)/(T_h - T_\ell) \le 0.2 \end{cases} \tag{6.7}$$

Obviously, in the static mode this measure is a function of time. The rate of stratification degradation increases with the increase in the rate of decrease of $F(t)$. This measure may also be applied in the dynamic mode of operation. For example, during the discharge of an initially stored hot water at T_h the outlet temperature is not allowed to drop below the useful temperature mentioned above. Likewise, for chilled water storage the outlet temperature is not allowed to rise above the useful temperature defined above. The transient outlet temperature profile is then used to calculate the cumulative discharge heating or cooling capacity, Q_d, as:

$$Q_d = \int_0^{t_d} \dot{m} C_p \left| T_e(t) - T_{in} \right| dt \tag{6.8}$$

The discharge time limit is now determined by the useful temperature as defined above. Also, the absolute value of the temperature difference is used to enable the equations to be valid for heat or cold storages. In the discharge mode the percent heat or cold recoverable as defined by Equation 6.3, now without the time dependence, is termed the *discharge efficiency*, η_d:

$$\eta_d = Q_d / Q_o \tag{6.9}$$

Clearly, η_d is dependent on the useful temperature considered, and therefore the useful temperature used should be quoted alongside. In the charging mode the charging efficiency is used.

The *charging efficiency* (also called the *storage efficiency*) is defined as the ratio of the net stored energy at the end of charging to the maximum energy that may be stored in a perfectly stratified tank, i.e. plug flow with no heat transfer between the hot and cold fluids:

$$\eta_c = Q_c / Q_o \tag{6.10}$$

where

$$Q_c = \int_0^{t_c} \dot{m} C_p \left| (T_e(t) - T_{in}) \right| dt \tag{6.11}$$

Again, the charging time limit, t_c, may be determined by the allowable outlet temperature. Wildin and Truman (1985a) defined the thermal efficiency of a chilled water storage tank for a full cycle of discharge and charge as the ratio of the integrated discharging to the integrated charging capacities, i.e.

$$\eta_{th} = Q_d / Q_c \tag{6.12}$$

where Q_c and Q_d are determined as before. For stratified chilled water storage in full-scale and scale-model tanks, cycle efficiencies ranging from 80–90% were obtained.

For the charge-discharge cycle thermal efficiency as defined by Equation 6.12 to be a valid performance indicator, it was pointed out by Wildin and Truman (1985a) that the temperature distributions in the tank at the end of discharge and at the start of charge should be identical. Failure to achieve this would result in a net heat addition or withdrawal, leading to inaccurate values of cycle efficiency. Also, the cycle efficiency does not account for internal heat transfer and mixing. The integrated cooling capacity of an initially charged tank would not recognize the effect of temperature blending. For this reason, and because it is always difficult in practice to duplicate the same experimental conditions, another measure of performance less sensitive to the initial temperature distributions was devised. This was called the *Figure Of Merit (FOM).* This index, first used by Tran *et al.* (1989) to evaluate the thermal performance of chilled water storage, was subsequently used by other investigators (Wildin, 1989; Wildin and Truman, 1989). It is defined as the ratio of the cooling capacity during the discharge (or equivalently, the energy added to the tank by the load) to the maximum cooling capacity theoretically available in the fully charged tank. This latter quantity is calculated based on the temperature difference between the average inlet temperature during discharging and the average inlet temperature during charging. Thus, the *FOM* is calculated by

$$FOM = \left[\sum \dot{m} C_p \left(T_{in} - T_e\right) \Delta t\right]_{discharge} / MC_p \left(T_{in,d} - T_{in,c}\right)_{average} \tag{6.13}$$

where M is the total mass of the water in the charged tank.

In the variable inlet temperature condition a measure termed the *mix number* (*MIX*) was devised by Davidson *et al.* (1994). *MIX* is based on the energy distribution level in the tank, and is determined by what is termed the *first moment of energy*, defined by analogy with the first moment of mass. That is, $M_E = \int_0^H y dE$ by analogy with $M_m = \int_0^L x dm$. M_E may be approximated by

$$M_E = \sum y_i E_i \tag{6.14}$$

where $1 < i \leq n$, and n is the number of uniform-temperature segments the tank is divided into, y_i is the distance from the center of the ith segment of volume $\forall_i$, to the bottom of the tank and $E_i = \rho \forall_i C_p T_i$. According to this definition, perfectly-stratified tanks have the largest M_E, while fully-mixed tanks have the smallest M_E and actual stratified tanks have a value in between. Thus, M_E may be used to characterize the stratification level in thermal storage tanks. The *mix number* is defined by the following dimensionless expression:

$$MIX = (M_{E,stratified} - M_{E,actual}) / (M_{E,stratified} - M_{E,fully-mixed}) \tag{6.15}$$

In view of Equation 6.14, the *mix number*, *MIX*, considers both the energy level and the temperature distribution. Clearly, the mix number is zero when an actual tank's performance approaches that of the perfectly stratified tank, i.e. $M_{E,actual} = M_{E,stratified}$ and it is unity when actual tanks are fully mixed. Also, because of the transient nature of the temperature profile the mix number varies with time. But this does not affect its usefulness when one is concerned with the relative performance of different tank designs under the same flow and thermal conditions. The three quantities in the above expression for *MIX* are determined using Equation 6.14 as follows: $M_{E,actual}$ is calculated from the measured temperature profile, $M_{E,stratified}$ and $M_{E,fully\text{-}mixed}$ are calculated based on the temperature profiles calculated from the perfectly-stratified and fully-mixed tank models (see section 6.4) respectively for the same actual test conditions. Using the mix number, Davidson *et al.* (1994) compared the performance of two inlet configurations under variable inlet temperature conditions. These inlets were a conventional inlet (drop-tube inlet located at the top of the tank) and a rigid porous manifold. The results for three different test conditions show lower values of *MIX* for the manifold inlet compared with the drop-tube inlet, indicating the consistency of *MIX* in measuring the stratification level achieved with different inlets. In the variable inlet temperature case, Philips and Dave (1982) used a coefficient which characterizes the effect of mixing in a stratified tank on the daily thermal performance of the solar energy collection system. A review of this and other measures may be found in Davidson *et al.* (1994).

Lately, exergy and exergy efficiency have been used to evaluate the performance of TES systems. Exergy is a measure of usefulness or quality of energy. It is defined as the maximum work potential of any particular form of energy in relation to its environment where this work is obtained by reversible processes. From the first and second laws of thermodynamics, the exergy of a material flow has the following form:

$$Ex = (h - h_a) - T_a\ (s - s_a) \tag{6.16}$$

The exergy of a heat flow is given by:

$$Ex = Q(T - T_a)/T \tag{6.17}$$

Here, h and s are the enthalpy and entropy, respectively, evaluated at the system temperature T and pressure p, while h_a and s_a are the enthalpy and entropy evaluated at the ambient temperature T_a and pressure p_a and Q is the heat transfer.

Rosen (1991) used energy and exergy efficiencies to examine the effect of temperature levels on the performance of a simple sensible TES system. A closed system was considered, involving only heat interactions: heat charge, heat discharge and heat losses to the environment. He defined the exergy efficiency as $\eta = Ex_d / Ex_c$, where Ex_d and Ex_c are obtained from Equation 6.17. Noting that the energy efficiency is $\eta = \eta_{th} = Q_d / Q_c$, an expression for the ratio ψ / η was derived as:

$$\psi / \eta = (T_d - T_a)\ T_c\ /\ (T_c - T_a)\ T_d \tag{6.18}$$

Here, T_c, T_d, and T_a are the charge, discharge, and ambient temperatures, respectively. He calculated the ratio ψ / η for different values of charging and discharging temperatures,

the results are given in Table 6.1. It is seen that the energy and the exergy efficiencies are equal only when the charging and discharging temperatures are equal, which is unachievable in practice. The energy and exergy efficiencies differ as T_d is decreased below T_c, and the difference becomes more pronounced as the difference between T_d and T_c increases. This shows the importance of temperature in performance evaluation of TES systems via exergy efficiency, which is sensitive to the temperatures at which heat is charged and discharged.

Rosen and Hooper (1991) evaluated the exergy contents of a stratified tank having water as the storage fluid, and a fixed energy content. The temperatures at top and bottom of the TES were held constant. The TES was subjected to three types of temperature distribution between these locations; linear, stepped and continuous-linear. From their evaluation, while the energy content was fixed, the values of exergy were different for the three types of temperature distribution. The system with more stratification had the highest value of exergy, and the least stratified had the lowest value of exergy. So, exergy gives a quantitative measure of stratification as it changes with the stratification level in the tank.

6.4 Experimental and Theoretical Foundations

The single stratified thermal storage tank has been the subject of numerous experimental and theoretical studies that were motivated in the early 1970s by solar energy storage applications. Brumleve (1974) confirmed the feasibility of using a natural thermocline to achieve separation of hot and cold water inside a single container. Many experimental and theoretical works have appeared since then. Lavan and Thompson (1977) experimentally studied the effect of several geometric and dynamic parameters, i.e. inlet port location and geometry, mass flow rate, tank height to diameter ratio, and the difference in temperature between the inflow and the liquid in the tank. Stratification was found to improve with increasing tank aspect ratio (height to diameter ratio), temperature difference and inlet port diameter. The increase in flow rate had an adverse effect on stratification. Best results were obtained when the inlet and outlet ports were located near the top and bottom walls and the flow was directed towards these walls.

For the same storage volume tall tanks maintain better stratification than short ones. Also, for the same thickness of the thermocline region less fluid in taller tanks is wasted to this intermediate temperature region. However, a limit exists as taller tanks tend to have a larger surface area per unit volume, thereby increasing the heat loss to the surroundings and the insulation cost.

Table 6.1 Values of the ratio ψ / η for a range of practical values of T_d and T_c (Rosen, 1991).

Discharging temperature,	Charging temperature, T_c(°C)			
T_d(°C)	40	70	100	130
40	1.00	0.55	0.40	0.32
70	-	1.00	0.72	0.59
100	-	-	1.00	0.81
130	-	-	-	1.00

The reference environment temperature is set at T_a = 10°C = 283 K.

To provide a high level of stratification without excessive thermal loss an aspect ratio of 4 was recommended by Cole and Bellinger (1982). A ratio of 10 was recommended by Abdoly and Rapp (1982). However, this value would result in a high surface area-to-volume ratio and subsequently increase the heat loss and the insulation cost. In their experiments with tanks with an aspect ratio of between 2.0 to 3.5, Nelson *et al.* (1999) found that improvements in thermal performance were negligible beyond an aspect ratio of 3.0. Analytical studies have shown that little improvement in stratification was achieved for an aspect ratio greater than 3.3 (Al-Najem *et al.*, 1993), and 4.0 (Ismail, *et al.*, 1997; Hahne and Chen, 1998). It was pointed out earlier by Lavan and Thompson (1977) that an aspect ratio between 3 and 4 constitutes a reasonable compromise between performance and cost.

Sliwinski *et al.* (1978) found that the position and sharpness of the thermocline are functions of the Richardson and Peclet numbers. A critical value of the Richardson, *Ri*, number of 0.244 was found to be the limit below which stratification does not occur. *Ri* was based on the tank height and the inlet flow velocity. The extent to which mixing occurs in stratified tanks as well as the design improvements to minimize it were investigated by Baines *et al.* (1982). Based on their experiments with fresh-saline and hot-cold water systems it was determined that there are two factors which limit the approach to ideal stratification: the critical layer thickness which defines the volume of fluid that must be introduced before mixing across the thermocline ceases, and the thermocline thickness. Both factors were found to be controlled by the design of the inlet system. To enhance thermal stratification several inlet designs were tested. Cole and Bellinger (1982) tested five different inlet designs. They concluded that the dual radial diffusers are the best. Also, they defined the best inlet design for the thermocline TES as that which introduces the flow horizontally at the top or bottom with minimum velocity. In order to maintain a high degree of stratification in solar collector systems the tank inlet temperature should remain constant. Accordingly, Cole and Bellinger (1982) recommended a new collection strategy that ensures a high degree of stratification. This strategy is based on limiting the flow through the tank to one tank turnover per day and controlling the flow rate to maintain a constant inlet temperature.

Because of the low thermal conductivity of water, conduction across the thermocline was found to be a minor factor in degradation of stratification as compared to other factors, i.e. mixing during the initial stages of charge and discharge, heat loss to the surroundings, and vertical conduction through the walls. One of the earliest studies of the effect of conducting wall on the decay of thermal stratification was that of Miller (1977). Experiments were conducted on two laboratory cylindrical tanks of slightly different sizes and with different wall materials: aluminum and glass. After establishing a thermocline by filling the lower half of the tank with cold water and introducing hot water at the top, temperature measurements along the centerline and at the side wall were taken as a function of time. The results indicate that the degradation of thermocline in the metal tank is six times greater than that in the glass tank. To explain this, Miller (1977) compared the measured temperature profiles with those calculated numerically for the case of heat diffusion across the thermocline. The discrepancy was too large, indicating heat transfer other than diffusion across the thermocline is responsible. This was the conduction along the wall cooling the hot liquid region close to the wall while warming that in the cold region. Consequently, a horizontal non-uniformity in temperature results, leading to buoyancy induced convective currents that enhance mixing and broaden the thermocline.

Noting that the thermal conductivity of water and glass are about the same, it was concluded that the tank wall must be made of a material of thermal conductivity not much greater than that of the stored liquid. Of course, smaller thermal conductivity is preferable. Later, Hess and Miller (1982) studied the effect of wall axial conduction on stratification decay by measuring the velocity field close to the wall using an LDV system. The heat diffusion through the thermocline and the heat loss to the ambient surroundings were isolated in these experiments. That is, the experiments were conducted on an initially uniform low-temperature water tank subjected to axial heat conduction that was obtained by imposing a constant temperature on the cross section of the tank vertical wall. The velocity measurements have shown clearly that for the conditions tested, convective currents are responsible for the degradation of thermocline.

The thermal decay of an initially stratified fluid in two plexiglass insulated rectangular tanks was investigated by Jaluria and Gupta (1982). Several initially stratified temperature distributions were established and the thermal decay was monitored in terms of the temperature distribution along the tank's vertical axis as a function of time and height for several values of the heat loss parameter, $S = UPH^2/A_c k$. Here U is the overall heat transfer coefficient, k is the fluid thermal conductivity, and P, H, and A_c are the tank perimeter, height, and cross-sectional area, respectively. The measured temperature distribution in static tests was found to exhibit horizontal uniformity. Although there was some variation close to the wall due to heat loss to the ambient surroundings, the buoyancy induced motion acts to re-establish the uniformity quickly. This was the basis used for justifying the one-dimensional heat conduction model developed by the authors. Also, the temperature distribution in the top region maintains vertical uniformity as it cools with time. This uniformity is attributed to the heat loss from the top, which cools the uppermost layer causing it to sink and mix with the fluid layers below. This process is repeated causing the average temperature of the initially high-temperature top region to decrease with time. The initially cold bottom region experiences an increase in temperature as a result of cooling the upper region close to the wall. This locally cooled fluid sinks down causing a mixing which leads to a fully mixed condition at the bottom region. The one-dimensional nature of the temperature distribution in a stratified TES tank was recognized from early studies (Close, 1967; Brumleve, 1974). The radial measurements of temperature distribution in a stratified tank has also confirmed this (Gross, 1982). Therefore, many of the one-dimensional modeling efforts find justification on this basis (see section 6.5).

It is clear that the degradation of the thermocline in static mode under partial charge or discharge is faster if the thermal conductivity of storage wall material is higher than that of the stored fluid. In such tanks it is recommended that an insulation layer be applied at the interior surface of the tank. In storage tanks made of concrete (Wildin and Truman, 1985a), stratification was maintained over a wide range of operating strategies of charge, discharge and recycling. The fluid-to- wall thermal conductivity ratio is the governing parameter. The higher this ratio the better the stratification.

The previous findings regarding the effect of the conducting wall were based on static tests with partially charged tanks. In the dynamic mode of operation the heat transfer through the tank wall was found to have a negligible effect on stratification (Lightstone *et al.*, 1989). Murthy *et al.* (1992) conducted experiments with three cylindrical scaled model tanks of the same internal diameter. Two of the tanks were made of mild steel of different thickness (1.0 and 2.4 mm) and the third one was made of aluminum of 1.0 mm thickness.

The three tanks were insulated with the same thickness of glass wool mats on all sides. Experiments covered both static and dynamic tests, with the latter tests covering both the discharge (only the load loop was on) and the simultaneous discharge and charge cycles (both the load and the heat source loops were on). Temperature measurements at ten locations along the axes of the tanks were taken at different time intervals. Their results demonstrated that thermocline decay is faster for the aluminum tank. At an inlet-to-outlet temperature difference of 48°C the extraction efficiency was about 5% less for the aluminum tank. This decrease is less at lower temperature differences. These results are in accord with the results of Lightstone *et al.* (1989).

The mixing introduced by the inflow during the charge and discharge was recognized as a major contributor to the degradation of the stored energy. Therefore, different inlet configurations were designed and tested. These designs may be classified into two categories: the constant-inlet temperature flow diffusers and the variable-inlet temperature flow distributors. These are shown in Figures 6.3 and 6.4 for the former and in Figure 6.5 for the latter. As stated earlier, the former condition is more common in chilled water storage and in solar energy collection systems with controlled output temperature. In this case inlets that introduce the flow with minimum velocity and in a gravity or surface current forms are the most effective in producing a thin thermocline. Extensive research on diffusers for chilled water storage was conducted by a group of researchers (see Wildin and Truman, 1985a; Wildin, 1990, 1991, 1996). Flow visualisation and temperature measurements in a laboratory-scale model chilled-water storage tank were conducted by Yoo *et al.* (1986). The tank was equipped with a linear-slot diffuser spanning one side of the tank bottom. Also, the slot height was variable to obtain different values of inlet flow Froude number. It was concluded that for better stratification the inlet densimetric Froude number, Fr, should not exceed 2, where Fr is based on the slot height and the average velocity of the flow from the slot. A value of unity or less was recommended by Wildin and Truman (1985b). By adding a settling mesh to single- and multi-tube diffusers, Al-Marafie *et al.* (1991) obtained better stratification with mesh than without it. Clearly, the design of the inlet in a thermocline TES tank is critical for better performance.

The effect of the inlet geometry on stratification in thermocline TES tanks was the subject of several research works carried out at Oklahoma State University. Using a fresh-saline water system, three radial diffusers of different geometry were tested by Zurigat *et al.* (1988). These were a solid disk radial diffuser, a perforated disk, and a perforated disk with a solid center. The tank, filled initially with fresh water, is charged with saline water from the bottom resembling the charge of a chilled water storage TES tank. Using a conductivity probe installed at the exit from the tank, the transient salt concentration profiles were obtained. The advantage of the experiments with a fresh-saline water system is the isolation of two stratification degradation mechanisms: the heat loss to the surroundings and the conduction along the tank wall. The results indicated that the perforated radial diffuser with a solid center gives the thinnest thermocline. Further experiments using a hot-cold water system were conducted by Zurigat *et al.* (1991) for the charging of a hot-water thermocline TES tank. Three inlet configurations were tested. These are the side inlet, the impingement inlet, and the perforated inlet (see Figure 6.4). Characterization of the mixing introduced by these inlets was carried out using an inlet mixing parameter introduced in a one-dimensional flow model (see section 6.5). The effect of the inlet geometry was also studied numerically by Zurigat (1988) (see also Ghajar and Zurigat, 1991) using a two-dimensional flow and heat-transfer model (see section 6.6).

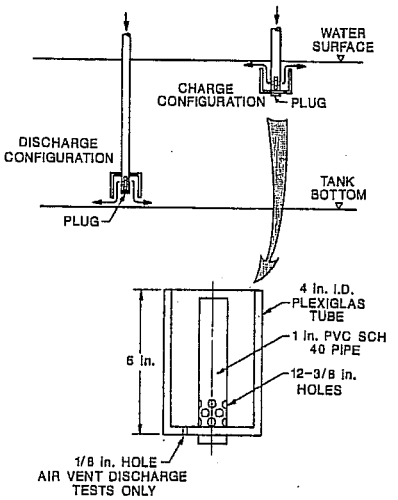

Figure 6.3 Schematics of the cup diffuser (Loehrke *et al.*, 1979).

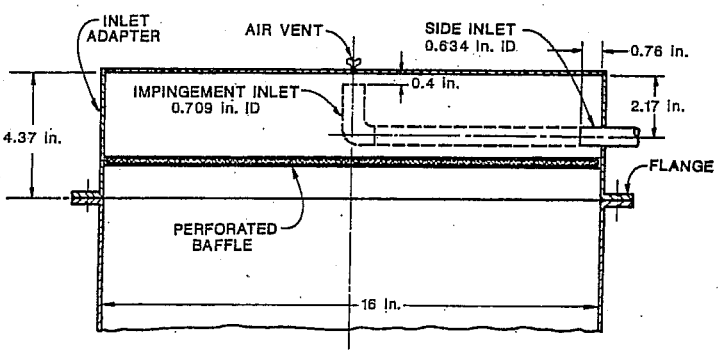

Figure 6.4 Schematics of the inlet configurations tested by Zurigat *et al.* (1991).

Most of the experimental work reported in the literature was conducted under constant inlet temperature, i.e. thermocline TES. The case of variable inlet temperature (stratified TES) has been studied in relation to solar energy collection systems. Inlets designed for the variable inlet-temperature case are termed *inlet distributors*. The common feature of these distributors is the use of perforated manifolds to house the incoming stream while allowing it to reach its temperature level where it exits the manifold through side perforations (see Figure 6.5). Notable design attempts are those which consist of rigid or flexible distribution manifolds (Sharp and Loehrke, 1979; Gari *et al.*, 1979; Davidson *et al.*, 1994; Davisdon and Adams, 1994), light flexible hose (Van Koppen *et al.*, 1979), rigid solid deflector baffles (Davis and Bartera, 1975), and rigid perforated distributor baffle (Abu-Hamdan *et al.*, 1992). Under variable inlet temperature the tests conducted with rigid porous manifolds have shown better performance than the conventional fixed inlets (Gari *et al.*, 1979). This was also shown by Davidson *et al.* (1994) by comparing the performance of a rigid porous manifold with a conventional drop-tube inlet. Under different test conditions the performance was monitored using the *mix number, MIX,* introduced in section 6.3. Despite their better performance the rigid porous manifolds are not in general use because of their

inflexibility in adapting to flow conditions other than those for which they are designed. A remedy was suggested by Davidson and Adams (1994), who designed a fabric manifold which they showed to be 4% more effective in maintaining stratification than rigid porous manifolds and 48% more effective than the conventional drop-tube inlet.

The inlet distributor of Abu-Hamdan *et al.* (1992) consisted of a perforated circular baffle with a solid portion located about its mid-height. The baffle was fitted inside the test tank resulting in an annulus space of 2.5 cm. The incoming flow enters the tank through 32 inlets located around the circumference of the test tank at mid-height. The flow then impinges on the solid portion of the baffle which in turn deflects it either up or down depending on the flow temperature. The deflected stream then flows through the perforated sections of the baffle. Tests using this distributor and two conventional inlets, a side and a drop-tube inlets, were conducted. It was concluded by Abu-Hamdan *et al.* (1992) that passive devices of the type used in their experiments or that used by Davis and Bartera (1975) offer no advantage over conventional inlets. More work in this area of distributor design for variable inlet-temperature conditions is still needed.

Theoretical studies of stratified TES tanks were conducted using one-, two- and three-dimensional models. The former two are discussed in the next two sections. Three-dimensional modeling efforts of stratified TES are scarce. The model of Sha and Lin (1978) is a notable model of this kind. Because of computer time limitations three-dimensional models are generally avoided despite their potential for assessing stratified TES tank design concepts.

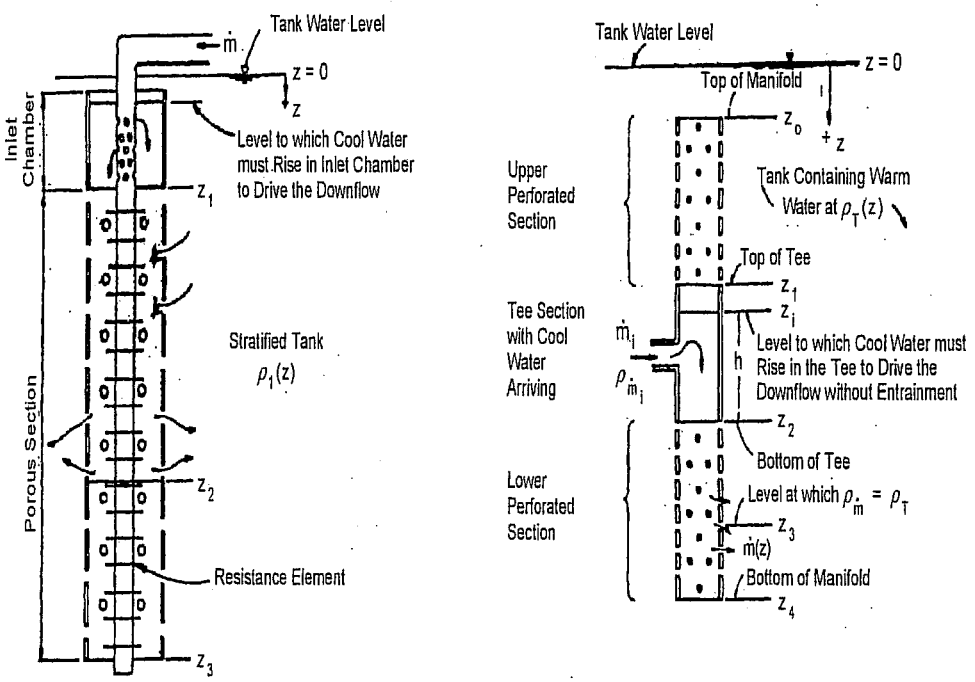

Figure 6.5 Stratified thermal storage tank inlet distributors (Gari *et al.*, 1979; Loehrke *et al.*, 1979).

6.5 One-Dimensional Models

The one-dimensional models of stratified thermal energy storage may be classified into two categories depending on the inlet temperature condition. These are the *stratified* TES tank models in which the inlet temperature is allowed to vary with time, and the *thermocline* TES tank models in which the inlet temperature is maintained constant. The latter condition results in a well-defined thermocline region of relatively small thickness. The former models were first developed for solar energy storage applications characterized by variable inlet temperature condition. In this section we discuss different one-dimensional models developed in the literature for both constant and variable inlet temperature conditions.

The *stratified* TES tank models represent a somewhat realistic condition between two idealized models of extreme cases that have, as discussed in section 6.3, utility in performance evaluation of thermal storage tanks and thermal storage systems. These are the *fully-mixed* and the *fully-stratified* tank models. In the *fully-mixed* model the entire liquid in the tank is assumed to have a uniform temperature which changes with time as a result of net energy addition or withdrawal during the charge or discharge processes or due to the interaction with the surroundings at T_a. The model equation representing this thermal balance may be written as:

$$MC_p \frac{dT}{dt} = \dot{m}_{in} C_p (T_{in} - T) - UA(T - T_a) \tag{6.19}$$

Equation 6.19 may be solved numerically for the initial condition *T(o)* equal to the average temperature of the liquid in the tank. In this equation M is the mass of water in the tank, T_{in} is the inlet temperature, $\dot{m}_{in}$ is the mass flow rate, A is the heat loss surface area, and U is the overall heat transfer coefficient. U may be found experimentally by measuring the rate of decay of initially heated water at uniform temperature in a static tank using Equation 6.21 below rearranged for U or UA. Typical values for hot water storage are $U = 0.973$ W/m^{2}K (Votsis *et al.*, 1988), $UA = 4.57$ W/K (Kleinbach *et al.*, 1993), and $UA = 2.7$ W/K (Davidson *et al.*, 1994). Alternatively, U or UA may be calculated based on forced and free convection correlations depending on the mode of operation, i.e. static or dynamic.

In the fully-stratified model the tank is subdivided into a number of uniform temperature layers and the inflow is assumed to seek its temperature level in the tank without exchanging heat with the adjacent layers or those along its path. The only heat interaction permitted is that with the surroundings at T_a. Under these conditions the energy balance for any layer, J, of mass M_J gives

$$M_J C_p \frac{dT_J}{dt} = -UA(T_J - T_a) \tag{6.20}$$

For an initial temperature $T_{o,J}$, the analytic solution of this equation over a time step, Δt, is

$$(T_J - T_a) = (T_{o,J} - T_a)\exp(-UA\Delta t / M_J C_p) \tag{6.21}$$

The temperature distribution in the storage tank can then be found by applying the solution given by Equation 6.21 to all the layers in the tank. However, during a time step, Δt, the incoming flow fills a finite volume which should be inserted in the tank in between two layers of higher and lower temperatures, respectively. To maintain continuity, the layers in

the tank are displaced up or down depending on whether the tank is in the charge or the discharge modes. For example, in the charge mode if the incoming stream is at temperature T_{in}, higher than that of the uppermost layer, then all the layers in the tank are displaced down resulting in the uppermost layer being filled with the incoming stream while the bottom layer exits the tank to the heat source. If T_{in} is somewhere between the two temperatures at the top and bottom layers, the incoming stream is placed in the tank at a location consistent with its temperature. That is, all layers with temperatures greater than T_{in} remain in place while those below are displaced downward. Again the lowest layer exits the tank to the source.

Turning to *stratified* TES tank models, the one-dimensional models of Close (1967), Duffie and Beckman (1980), and Sharp (1978) assume that the flow seeks its temperature level without mixing along its path. In addition, heat loss to the surroundings and mixing with the adjacent layers is allowed. These one-dimensional models were compared by Kuhn *et al.* (1980) by validation with experimental data, and the model of Sharp (1978) was found to give better predictions. Therefore, the latter model is discussed below along with the one-dimensional model of Han and Wu (1978) (known as the *Viscous Entrainment Model*) in which the above assumptions hold except the flow is now assumed to entrain fluid from the layers along its path

In the model of Sharp (1978), which allows for arbitrary variation in fluid inlet temperature, the tank is divided into a number of isothermal, constant volume segments. Energy and mass balance equations are written for each segment while accounting for thermal losses to the surroundings and vertical conduction through the tank walls. Using control functions the inlet fluid is directed to the segment whose temperature most closely matches its temperature without mixing with the segments along its path. However, mixing with the adjacent layers is allowed. Although the model does not explicitly account for turbulence, the number of segments used in the model has an effect on the calculated temperature profile similar to that due to turbulent mixing. This can be seen in Figure 6.6, which shows the temperature profiles calculated for different numbers of segments, N, under a constant inlet temperature. Higher N values result in predictions closer to ideal stratification or, equivalently, less mixing.

Han and Wu's (1978) *Viscous Entrainment* model is a finite-difference model that accounts for heat loss to the surroundings and the mixing effects due to entrainment of the tank fluid by the incoming stream. Also, collector and load flow circuits are incorporated and mass and energy balance equations are derived for both circuits and solved using an implicit finite-difference method. An additional equation describing the rate of viscous entrainment is also provided. A boundary condition parameter, γ, is introduced to account for mixing in the upper and lower regions of the tank due to the introduction of collector flow and load flow, respectively. The calculated transient temperature profiles, at a fixed location in the tank with different values of γ, are shown in Figure 6.7. It is seen that as γ increases the thermocline widens as expected. However, as γ increases beyond 20, unrealistic mixing takes place from one side of the thermocline. That is, the thermocline fronts for different values of γ are at the same location in the tank irrespective of the severity of the mixing at the inlet. Note that the results shown in Figures 6.6 and 6.7 were obtained under constant inlet temperature conditions. It is easier to visualize the validity of these models in this limiting case for the inlet flow condition.

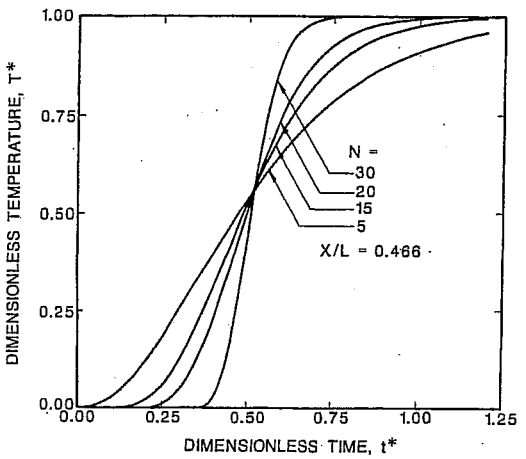

Figure 6.6 Effect of number of segments, N, on thermocline predictions using the model of Sharp (1978) (Zurigat *et al.*, 1989).

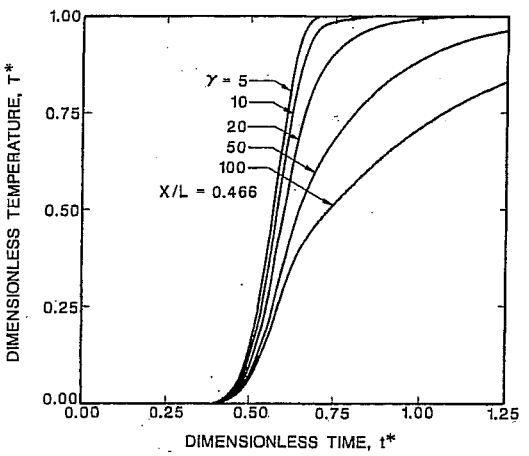

Figure 6.7 Effect of boundary condition mixing parameter, γ, on thermocline predictions using the model of Han and Wu (1978) (Zurigat *et al.*, 1989).

The fact that these models are also applicable to the thermocline TES case makes them more general than the thermocline TES models discussed next. However, in the thermocline TES case, simpler and more accurate models have been developed. The thermocline TES models are based on solving the one-dimensional convection-diffusion equation. This equation can be derived using an energy balance on the control volume shown in Figure 6.8, which represents a fluid region of uniform temperature subject to heat loss to the ambient surroundings through the tank wall and insulation. It is assumed that the flow is one-dimensional, i.e. the velocity is uniform over the tank cross section. In a tank with properly designed inlet and outlet diffusers this assumption of plug or piston-like flow is valid for most of the tank except at and in the vicinity of the diffusers, where the flow may be three-dimensional and turbulent. Furthermore, the thermo-physical properties of the

fluid are assumed constant and the thermal inertia of the tank wall and insulation negligible. Justification for the latter assumption has been demonstrated by Gretarsson *et al.* (1994). Then, the resulting energy equation of laminar flow is:

$$\frac{\partial T}{\partial t} + V\frac{\partial T}{\partial x} = \alpha\frac{\partial^2 T}{\partial x^2} + \frac{UP}{A_c\rho C_p}(T_a - T) \tag{6.22}$$

In this equation A_c is the cross-sectional area of the tank, V is the mean vertical velocity in the tank (based on A_c), U is the overall heat transfer coefficient, and P is the tank perimeter. Although Equation 6.22 seems simple to solve numerically, two potential problems arise. First, the flow experiences mixing at the inlet which is not taken into account in Equation 6.22. Second, unless care is taken, the stability of the numerical solution demands the use of the highly dissipative upstream differencing scheme, thereby compromising the accuracy. These two problems were treated by the model developed by a research group led by Professor Ghajar, which is referred to henceforth as the Ghajar model (Oppel *et al.*, 1986; Zurigat *et al.*, 1988; Zurigat *et al.*, 1991). The turbulent mixing was accounted for by introducing into Equation 6.22 an effective diffusivity factor, ε_{eff}, defined as

$$\varepsilon_{eff} = (\alpha + \varepsilon_H)/\alpha \tag{6.23}$$

Note that for laminar flow the eddy diffusivity for heat $\varepsilon_H = 0$ everywhere and $\varepsilon_{eff} = 1$. For turbulent flow ε_{eff} is much greater than unity. Multiplying the molecular thermal diffusivity in Equation 6.22 by this factor is equivalent to stating that the molecular thermal diffusivity, α, is magnified by turbulence by a factor of ε_{eff}. Equation 6.22 then becomes

$$\frac{\partial T}{\partial t} + V\frac{\partial T}{\partial x} = \alpha\varepsilon_{eff}\frac{\partial^2 T}{\partial x^2} + \frac{UP}{A\rho C_p}(T_a - T) \tag{6.24}$$

A finite-difference solution technique is used to solve Equation 6.24 subject to the appropriate initial and boundary conditions. The heat losses from the top and bottom of the tank are neglected. To ensure stability of the numerical solution of Equation 6.24 under all flow rates, the first space derivative should be descretized using the upwind difference representation. However, this representation produces numerical diffusion which results in inaccurate results. Therefore, to eliminate the numerical diffusion inherent in the upwind differencing of the first space derivative (convective term), Equation 6.24 is separated into two cases. These are the diffusion case

$$\frac{\partial T}{\partial t} = \alpha\varepsilon_{eff}\frac{\partial^2 T}{\partial x^2} + \frac{UP}{A_c\rho C_p}(T_a - T) \tag{6.25}$$

and the convection case

$$\frac{\partial T}{\partial t} + V\frac{\partial T}{\partial x} = 0 \tag{6.26}$$

An implicit finite-difference representation of Equation 6.25 yields the following:

$$\begin{aligned}(-\varepsilon_{eff}\,Fo)T'_{n-1} + (1 + \phi + 2\varepsilon_{eff}\,Fo)T'_n \\ + (-\varepsilon_{eff}\,Fo)T'_{n+1} = \phi T_\theta + T_n\end{aligned} \tag{6.27}$$

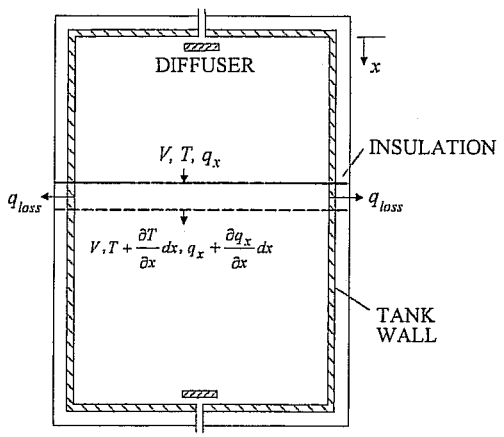

Figure 6.8 Energy balance in thermocline thermal energy storage tank.

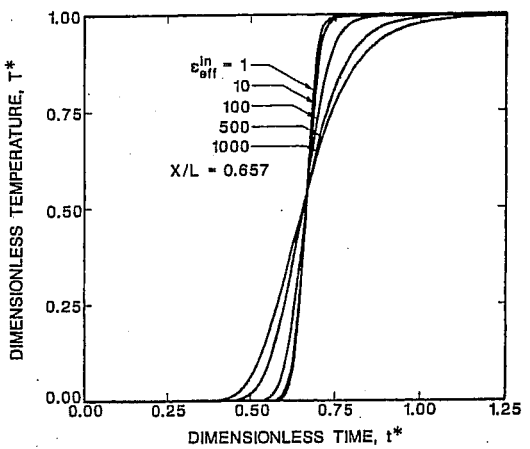

Figure 6.9 Effect of inlet effective diffusivity factor ε_{eff}^{in} on thermocline predictions using the model of Ghajar (Zurigat *et al.*, 1991).

Here, $\phi = U P \Delta t / A_c \rho C_p$ and Fo is the Fourier number; $Fo = \alpha \Delta t/(\Delta x)^2$. An explicit finite-difference representation of Equation 6.26 gives

$$T''_n = T_n - \frac{V \Delta t}{\Delta x} \left(T_n - T_{n-1} \right) \tag{6.28}$$

Here the double prime denotes new values that may be calculated at a time step different from that in Equation 6.27. To obtain the exact solution of Equation 6.28, the Courant number, $C = V\Delta t / \Delta x$, should be equal to unity. This gives

$$T''_n = T_{n-1} \tag{6.29}$$

For the variable flow rate case, C can be different from unity. Therefore, the 'buffer tank' concept (Oppel *et al.*, 1986) is used. This mathematical concept is based on setting the Courant number, C, equal to unity by the choice of Δx or Δt for the maximum expected flow rate, and applying Equation 6.29 only at multiples of Δt for which C is equal to unity for other flow rates. For example if $C = 1/2$, Equation 6.29 would be applied at every other time step.

The variation of ε_{eff} in Equation 6.27 needs to be specified. Since different inlets promote turbulence in varying degrees, it is expected that ε_{eff} will assume different values for different inlets. Based on experiments with fresh-saline water systems (Oppel *et al.*, 1986; Zurigat *et al.*, 1988), ε_{eff} was found to vary spatially from a maximum at the inlet ε'''_{eff} to a minimum of unity at the outlet in a decreasing hyperbolic function of the form (other functions were also tried, i.e. linear and exponential)

$$\varepsilon_{eff} = A / N_{sl} + B \tag{6.30}$$

where

$$A = (\varepsilon^{in}_{eff} - 1) / \left(1 - \frac{1}{N_{slt}}\right)$$

$$B = \varepsilon^{in}_{eff} - A$$

Here, N_{sl} is the slab number in increasing order from the inlet and N_{slt} is the total number of slabs, determined by

$$N_{slt} = H / (V \Delta t) \tag{6.31}$$

A problem thus remains in specifying the inlet value of the effective diffusivity factor, ε'''_{eff}. Figure 6.9 shows the model's predictions of the transient temperature profiles at a certain location in the tank *(X/L = 0.657)* for different values of ε'''_{eff} for an arbitrary condition. It is seen that the thermocline gets thicker as ε'''_{eff} increases. Despite its artificial nature, the effective diffusivity factor can represent the modifying effect of turbulence caused by the inlet flow. Hence, this factor may be used to characterize the inlet geometry and identify the best inlets. This feature has been demonstrated by Zurigat *et al.* (1988 and 1991). The variation of the inlet effective diffusivity factor as a function of the flow parameters, i.e. the ratio *Re/Ri*, is shown in Figure 6.10 for three different inlet configurations. Here, *Re* is based on the inlet port diameter, while *Ri* is based on the height of the tank, and both are based on the inlet port flow velocity. The three inlets used are the side inlet, the perforated inlet, and the impingement inlet (see Figure 6.4). As expected, the side inlet introduces the highest level of turbulence and mixing. The curves shown in Figure 6.10 are represented by the following correlations:

$$\varepsilon^{in}_{eff} = 0.344 \left(\mathrm{Re}/\, Ri\right)^{0.894} \quad \text{for the side inlet} \tag{6.32}$$

$$\varepsilon^{in}_{eff} = 3.54 \left(\mathrm{Re}/\, Ri\right)^{0.586} \quad \text{for the perforated inlet} \tag{6.33}$$

$$\varepsilon^{in}_{eff} = 4.75 \left(\mathrm{Re}/\, Ri\right)^{0.522} \quad \text{for the impingement inlet} \tag{6.34}$$

The above correlations were incorporated into the Ghajar model which was then confirmed by Zurigat *et al.* (1991) using experimental data from the literature and of their own research. Figures 6.11–6.13 show the predictions compared with the experimental data. The agreement between the predictions and the experiments is good. Thus, the introduction of the effective diffusivity factor has proved to be a powerful tool in modeling the mixing in thermocline TES tanks.

The model of Ghajar described above was compared with five one-dimensional models from the literature by Zurigat *et al.* (1989). The comparison was conducted with respect to experimental data from their own research and the literature for the constant inlet temperature condition, i.e. thermocline TES. The models considered were those of Sharp (1978), Han and Wu (1978), Cole and Bellinger (1982), Cabelli (1977) and Wildin and Truman (1985b). The tank modeled was assumed to be insulated with no wall axial conduction and no thermal inertia for the tank envelope. The first two models are described above and the other three below. The comparison showed varying degrees of agreement with thermocline test data. Generally, the best agreement was obtained by the models of Wildin and Truman (1985b), Cole and Bellinger (1982), and the model of Ghajar. Some adjustment of the parameters is needed in the former two models, while in the latter no adjustment is required in view of the correlations presented in Equations 6.32–6.34.

The model of Cole and Bellinger (1982) is a one-dimensional analytical model with empirically derived parameters. These are the mixing parameter, C, which accounts for mixing due to the introduction of fluid into the tank, the normalized film heat-transfer coefficient, H, which accounts for the fluid-wall thermal interaction, and the capacity ratio, a, which accounts for the effect of wall thermal inertia on stratification. For thin walls $a = 1$. The heat loss to the surroundings is neglected and the model is restricted to a constant flow rate and a constant inlet temperature, as well as a uniform initial temperature distribution. Zurigat *et al.* (1989) found that the parameter C has a significant influence on the thermocline shape, as shown in Figure 6.14, while the parameter H was found to have a negligible effect. Cole and Bellinger (1982) correlated the former parameter with the Fourier and Richardson numbers. The model of Cabelli (1977) is a closed-form solution of the one-dimensional energy equation with heat loss to the environment. No mixing effects are included.

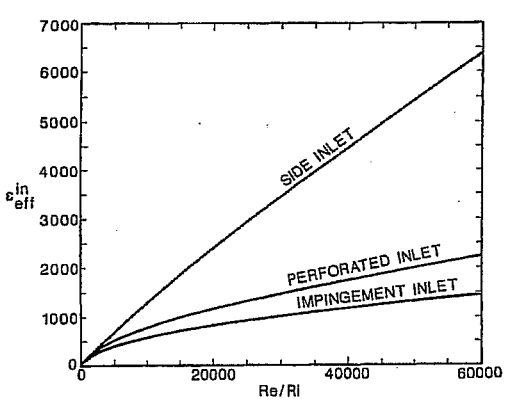

Figure 6.10 The variation of the inlet effective diffusivity factor ε_{eff}^{in} as a function of the ratio *Re/Ri* (Zurigat *et al.*, 1991).

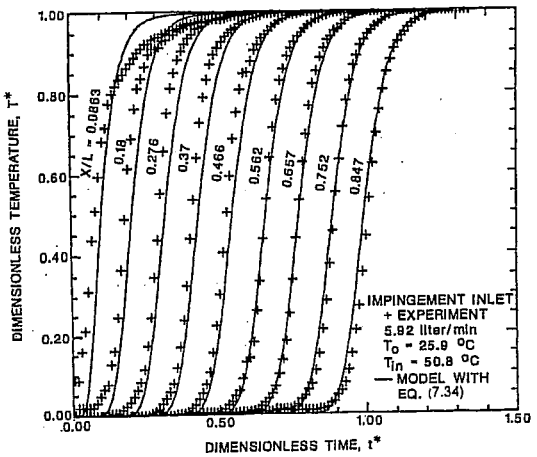

Figure 6.11 Predicted transient temperature profile at different locations in the storage tank using the model of Ghajar for the impingement inlet compared with the experiments (Zurigat *et al.*, 1991).

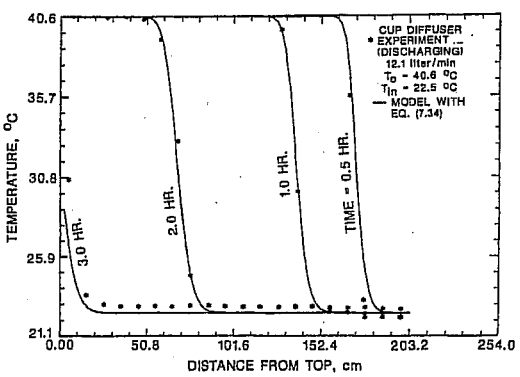

Figure 6.12 Predicted temperature profiles using the Ghajar model compared with the experimental data of Kuhn *et al.* (1980) for the discharge mode using the cup diffuser (Zurigat *et al.*, 1991).

The model of Wildin and Truman (1985b) is a finite-difference model that accounts for mixing at the inlet region, vertical conduction through the tank wall and water, the thermal capacitance of the tank wall and heat exchange with the surroundings. Mixing in the inlet is quantified by averaging the temperatures of a specified number of liquid elements, *NM*, near the inlet. Figure 6.15 shows the effect of the variation of *NM* on the thermocline. Based on experiments with chilled water storage, Wildin and Truman (1985a) concluded that the thickness of the mixing layer for well designed inlet diffusers was no more than 7% of the water depth, up to a maximum of 0.31 m. A well designed diffuser was defined as that which introduces the fluid into the tank in a gravity current flow at the bottom of the tank for cooler water and a surface current flow at the top of the tank for warmer water. A poorly designed diffuser is one which introduces the fluid in a jet-like form. Gretarsson *et al.* (1994) considered the depth of the mixing zone to be 3% of the tank depth for well-designed diffusers and 8% for poorly designed ones. These values are empirically-derived, and thus may differ from one investigator to another.

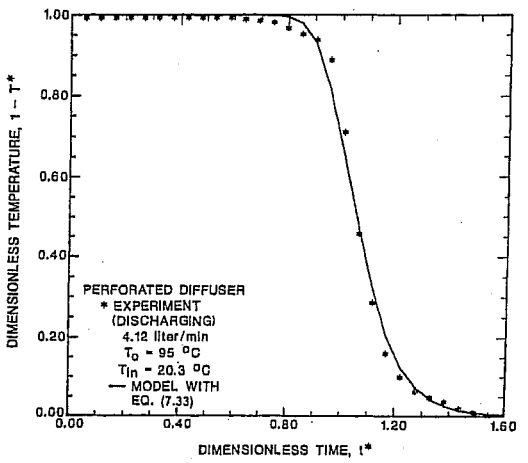

Figure 6.13 Predicted outlet temperature profiles using the model of Ghajar compared with the experimental data of Abdoly (1981) (Zurigat *et al.*, 1991).

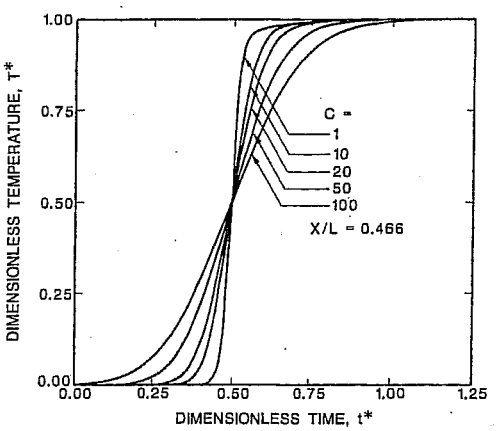

Figure 6.14 Effect of the mixing parameter, *C*, on thermocline predictions using the model of Cole and Bellinger (1982) (Zurigat *et al.*, 1989).

The concept of splitting the governing one-dimensional energy equation used in the Ghajar model was later adopted by other investigators. Votsis *et al.* (1988) assumed a constant eddy diffusivity (or mixing) factor and solved the equations for an insulated tank using an explicit finite difference method. Gretarsson *et al.* (1994) also used the same technique, which they called the 'discrete-time-step' model. The diffusion and heat loss terms in the transient heat conduction equation were discretized for each node and the resulting system of first-order differential equations was solved using the Runge-Kutta method. As with the Ghajar model, the time step and the number of finite fluid elements were determined from the Courant number by setting it to unity. Mixing, however, was introduced in the same way as that used by Wildin and Truman (1985b). That is, a mixing coefficient defined in terms of the percent of the total tank volume was introduced, representing the volume of water in the inlet region that should be mixed with the incoming

stream. This coefficient depends on the type of diffuser used. Although the Gretarsson *et al.* (1994) model ignores the tank wall thermal capacitance, they applied their model to concrete tanks of different thickness and compared their results with the predictions of the model of Wildin and Truman (1985b), which accounts for the thermal inertia of the tank walls. The comparison, expressed in terms of the relative difference in the calculated change in internal energy of the water for the two models, showed that ignoring the thermal capacitance introduces a difference of less than 3%. Based on this result, one-dimensional models that ignore the thermal inertia of the tank wall may find justification.

The localized mixing as used by Wildin and Truman (1985b) and Gretarsson *et al.* (1994) was also used in a different way by Nakahara *et al.* (1988), who assumed that the tank consists of two regions: a fully mixed region which increases in extent as filling proceeds, and a plug flow region spanning the rest of the tank. The extent of the fully mixed region was expressed in terms of a dimensionless depth $R = X/H$, where H is the tank height and X is the depth. R was assumed to vary linearly with the dimensionless filling time t^* ($t^* = Vt/H$) as:

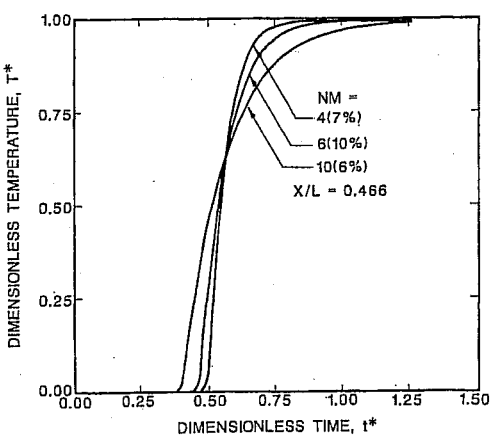

Figure 6.15 Effect of number of mixed segments, *NM*, on thermocline predictions using the model of Wildin and Truman (1985b) (Zurigat *et al.*, 1989).

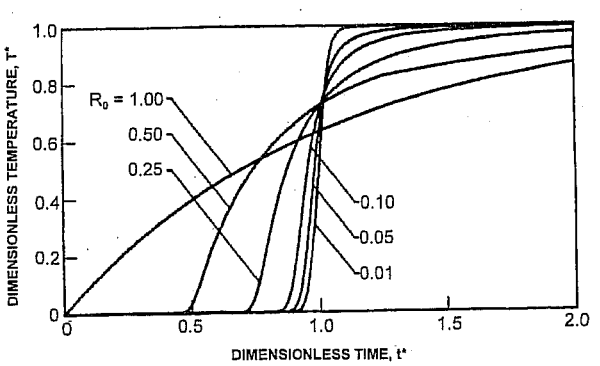

Figure 6.16 The outlet temperature profile predicted by the model of Nakahara *et al.* (1988).

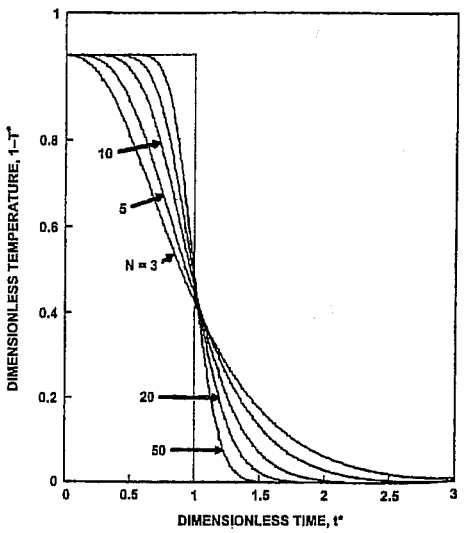

Figure 6.17 Predictions of storage tank outlet temperature profile using the layers-in-series model for different numbers of layers (Mavros *et al.*, 1994).

$$R = R_o + R_k t^* \tag{6.35}$$

where R_o and R_k are empirical constants. R_k was taken to be 0.4 under all conditions while $R_o = X_o/H$ represents the initial extent of mixing and its value depends on the inlet diffuser type and the inlet flow conditions. Correlations for R_o in terms of Richardson number and the inlet length scale were given for two different inlet types: a pipe inlet and a slot inlet. In the fully mixed region, Equation 6.19 with $U = 0$ is applicable. In terms of the volume of the tank the solution over the time interval Δt becomes:

$$T(t+\Delta t) = T_{in} + (T_o - T_{in}) \exp(-\dot{\forall}\Delta t / \forall_T R) \tag{6.36}$$

In the plug flow region the governing equation is the one-dimensional convection-diffusion equation which is solved numerically. The temperature profiles for different values of R_o are shown in Figure 6.16.

Another thermocline TES model called the *Layers-in-Series* model was developed by Mavros *et al.* (1994). The tank is subdivided into a number of uniform temperature layers and Equation 6.19 without heat loss to the surroundings is written for each layer. The resulting system of first-order ordinary differential equations is then solved in closed form. The inlet temperature of each layer was taken to be that of the upstream layer. Again, the number of layers has an effect on the temperature profile similar to that of mixing and diffusion. Figure 6.17 shows the transient outlet temperature profile predicted by the *Layers-in-Series* model for different numbers of layers. The unrealistic symmetry exhibited by the temperature profile predicted by this model (see Figure 6.17) motivated Mavros *et al.* (1994) to modify their model by adding to each layer a small side tank. Part of the flow entering each layer is diverted into its corresponding side tank and, by continuity, an equal amount is allowed to leave and enter the next layer downstream which experiences a similar flow diversion. To model this flow arrangement two empirical parameters were

devised to control the size of the side tank and the flow rate of the stream entering it. Then, energy balance equations are derived for each layer and each side tank, resulting in twice the number of equations used in *Layers-in-Series* model. The resulting system of equations is then solved numerically. As with all one-dimensional models the predictions depend on how well the empirical parameters are correlated with the flow conditions.

The effective diffusivity factor introduced in the model of Ghajar was also used in the same way by Al-Najem and El-Refaee (1997), who assumed it to vary in a spatially decreasing exponential function having a maximum value at the inlet which is correlated with the ratio of Reynolds to Richardson numbers. They solve Equation 6.24 without the heat loss term using a finite-element-based method known as Chapeau-Galarkin method. Homan *et al.* (1996) also used the same approach adopted in the model of Ghajar for quantifying the mixing in the thermocline TES tank. That is, using suitable time and space scales, Equation 6.24 is made dimensionless resulting in the diffusion term being multiplied by the inverse of an effective Peclet number, $Pe_{H,eff} = VH/(\alpha+\varepsilon_H)$. In terms of Peclet number $Pe_{H,eff} = Pe_H/\varepsilon_{eff}$. Then Equation 6.24 without the heat loss term is solved in closed form using Laplace transforms. This solution transposed explicitly for the effective Peclet number gives the functional relation used to determine the ratio ε_H/α (which is one less than ε_{eff}) from experimental data. This method assumes uniform mixing throughout the tank. As pointed out by Musser and Bahnfleth (1998), this assumption oversimplifies. Figure 6.18 gives the ratio ε_H/α as a function of Peclet number, Pe_H, for different inlet configurations. The dimensionless parameter T^*_{max} cited in Figure 6.18 is the maximum outlet temperature allowed by the load, and is given for the discharge mode by $T^*_{max} = (T_{max} - T_o)/(T_{in} - T_o)$. Figure 6.18 shows a good correlation, reinforcing the usefulness of the effective diffusivity factor introduced in the model of Ghajar. The results presented in Figures 6.10 and 6.18 for the effective diffusivity factor differ (in the order of magnitude) because those of Figure 6.10 are for the value at the inlet which is the maximum value while those of Figure 6.18 are the average uniform values.

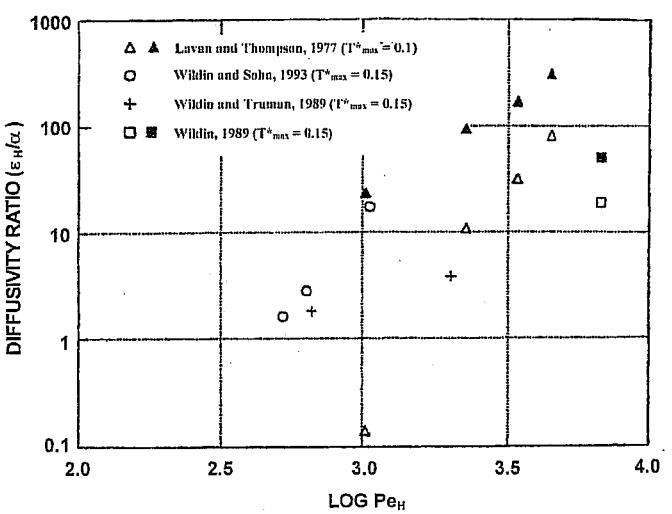

Figure 6.18 Empirical diffusivity ratios for stratified solar and chilled water storage tanks (Homan *et al.*, 1996).

Based on the foregoing, it is seen that the one-dimensional modeling has been the focus of many researchers because of its role in simulations of overall energy systems involving thermal storage. The problem of mixing introduced by the inflow has been treated in different ways, and is empirically based by the nature of one-dimensional modeling.

6.6 Two-Dimensional Models

In these models the conservation equations of flow and heat transfer in stratified thermal storage tanks are the two-dimensional continuity, momentum, and energy equations. In comparison with one-dimensional modeling, two-dimensional modeling involves less assumptions and empiricism, and thus is more realistic and accurate. A wider range of flow thermal and hydrodynamic conditions as well as complex tank geometric parameters may be modeled. Naturally, in addition to the increased computational effort in terms of formulation, programming and output data reduction, more computer time is required. This usually makes two-dimensional models unsuitable when the aim is to study the performance of energy systems involving thermal storage. The two-dimensional modeling of stratified TES has been conducted by several researchers. It should be mentioned at the outset that in solving the governing conservation equations of mass and momentum they are either left in their premitive-variables form or put in the vorticity-stream function form. Retaining the usual variables, the former form requires the solution of the pressure field using different algorithms depending on the numerical method used. For example, the SIMPLE algorithm (Patankar, 1980) and its upgraded versions or the Newton-Raphson pressure-adjustment algorithm (Hirt *et al.*, 1975). The second form has the advantage of identically satisfying the continuity by the stream function and eliminating the pressure by the cross product of the momentum equations. Furthermore, since the problem is of the mixed convection type, the Boussinesq approximation is used by all investigators. In this approximation the density is assumed constant except in the appropriate gravity term in the momentum equations. Also, unless otherwise stated, in the studies discussed below adiabatic conditions are assumed, and no localized resistance terms (baffles) are used. Finally, these numerical studies share the common objective of studying the influence of different design parameters on stratification such as the inlet port type and location, the flow direction, and the Reynolds and Richardson numbers effects.

The general two-dimensional flow and heat transfer model may be derived by assuming two-dimensional turbulent flow with negligible viscous dissipation, and with the Boussinesq approximation invoked. Then, the governing equations written in primitive variables and in conservative form in both Cartesian ($\xi = 0$) and cylindrical coordinates ($\xi = 1$, $x = r$) reduce as follows:

- Continuity:

$$\frac{\partial u}{\partial x} + \frac{\partial v}{\partial y} + \xi \frac{u}{x} = 0 \tag{6.37}$$

- x- and y-momentum:

$$\frac{\partial u}{\partial t}+\frac{\partial uu}{\partial x}+\frac{\partial uv}{\partial y}+\xi\frac{u^2}{x}=-\frac{1}{\rho_o}\frac{\partial p}{\partial x}+\frac{\partial}{\partial x}\left(\frac{\mu_{eff}}{\rho_o}\frac{\partial u}{\partial x}\right)+\frac{\partial}{\partial y}\left(\frac{\mu_{eff}}{\rho_o}\frac{\partial u}{\partial y}\right)$$
$$+\xi\left[\frac{\mu_{eff}}{x\rho_o}\left(\frac{\partial u}{\partial x}-\frac{u}{x}\right)\right]-\frac{R_x}{\rho_o l_x} \qquad (6.38)$$

$$\frac{\partial v}{\partial t}+\frac{\partial uv}{\partial x}+\frac{\partial vv}{\partial y}+\xi\frac{uv}{x}=-\frac{1}{\rho_o}\frac{\partial p}{\partial y}+g_y\beta(T-T_o)+\frac{\partial}{\partial x}\left(\frac{\mu_{eff}}{\rho_o}\frac{\partial v}{\partial x}\right)$$
$$+\frac{\partial}{\partial y}\left(\frac{\mu_{eff}}{\rho_o}\frac{\partial v}{\partial y}\right)+\xi\frac{\mu_{eff}}{x\rho_o}\frac{\partial v}{\partial x}-\frac{R_y}{\rho_o l_y} \qquad (6.39)$$

- Energy:

$$\frac{\partial T}{\partial t}+\frac{\partial uT}{\partial x}+\frac{\partial vT}{\partial y}+\frac{\xi}{x}uT=\frac{\partial}{\partial x}\left(\frac{k_{eff}}{\rho_o C_p}\frac{\partial T}{\partial x}\right)+\frac{\partial}{\partial y}\left(\frac{k_{eff}}{\rho_o C_p}\frac{\partial T}{\partial y}\right)+\xi\frac{k_{eff}}{x\rho_o}\frac{\partial T}{\partial x} \qquad (6.40)$$

The effective viscosity and conductivity appearing in the governing equations are defined as the sum of the laminar and turbulent contributions, i.e.

$$\mu_{eff}=\mu_t+\mu_t$$
$$k_{eff}=k_t+k_t \qquad (6.41)$$

where μ_t and k_t are the turbulent contributions obtained from a suitable turbulence model. Two simple turbulence models are presented at the end of this section. The resistance terms, R_x and R_y, arise due to the presence of solid or perforated obstructions in the flow field, and are defined by Sha and Lin (1978) as

$$R_x=\frac{1}{2}f\rho|u|u$$
$$R_y=\frac{1}{2}f\rho|v|v \qquad (6.42)$$

where the friction factor is calculated based on the diameter and thickness of the perforations. The symbols l_x and l_y appearing in the resistance terms are the appropriate length scales associated with R_x and R_y, respectively. l_x and l_y are taken as the grid sizes in the x and y directions, respectively.

The numerical solution of the above equations, which are highly non-linear and coupled partial differential equations, has been the subject of several studies. These studies, however, differ depending on the assumptions and the numerical methods used. One of the earliest computational studies of stratified thermal storage in dynamic mode was that of Cabelli (1977). The conservation equations in cartesian coordinates and in vorticity-stream function formulation were solved using an implicit finite-difference method. All convective derivatives were discretized using a central-difference representation which is known to lead to instability at high Reynolds numbers. This limited the solution to Reynolds numbers

of 200 or less where *Re* (also *Ri*) was based on the inlet port velocity and the height of the tank. The study simulated both vertical and horizontal inflow and outflow. Also, single-flow (charge or discharge) and two-flow (charge and discharge) circuits operating simultaneously were simulated. Although limited in applicability in view of the low *Re* used, the results demonstrated the role of the Richardson number *Ri* in achieving stratification. Increasing *Ri* beyond unity was shown to have a negligible effect on stratification. One has to keep in mind the definition of the Richardson number in light of the reference quantities used. Chan *et al.* (1983) solved the same equations, in primitive variables, using an explicit finite difference method. Different inflow and outflow configurations were simulated. However, their results showed that the flow direction into and from the storage tank has little effect on thermal storage efficiency, contrary to the experimental evidence.

The limitation on Reynolds number values in Cabelli (1977) was later removed by Guo and Wu (1985), who solved the same equations, again in vorticity-stream function formulation, using a finite difference method with a power-law scheme (Patankar, 1980) for the convective derivatives. Thus stability was secured at high values of Reynolds number. However, this method is known to produce numerical diffusion, which compromises the accuracy. As in the study of Cabelli (1977), the Richardson number *Ri* was identified by Guo and Wu (1985) as the important parameter for characterizing the flow pattern and temperature distribution inside the storage tank. For a single-flow circuit, values of $Ri > 1$ were found to provide better stratification. *Ri* is based on the tank height and the inlet velocity. For the case of two-flow circuits, poor stratification was obtained at $Ri = 1$. In an attempt to improve thermal stratification, Han and Wu (1985) incorporated in their numerical study a horizontal baffle located at a distance of one fourth the height of the tank from the bottom and extending slightly beyond the middle of the tank. Simulations of discharge of an initially hot water tank with and without a baffle showed varying degrees of improvement depending on Richardson number. That is, for $Ri < 1.2$ the improvement was excellent and it was good for $Ri = 1.2$, whereas for $Ri > 2.4$ the improvement was marginal. At Richardson numbers of 9.8 or higher the baffle was found to give negligible improvement on stratification. The foregoing results were for laminar flow. Han and Wu (1985) also used a simple eddy viscosity model of mixing length type, and found little difference in the qualitative behavior compared with that predicted by the laminar flow calculations.

Later, Zurigat (1988) (see also Ghajar and Zurigat, 1991) solved the two-dimensional model equations in primitive variables using the numerical solution algorithm of Hirt *et al.* (1975) known as the SOLA algorithm. The model incorporated both cylindrical axisymmetric and cartesian coordinates, laminar and turbulent flows, constant and variable boundary conditions, and localized resistances in the form of perforated and solid baffles of zero thickness. Also, both the weighted upwind and the second-order upwind difference schemes were implemented for all equations. The latter upwind scheme was used to reduce the numerical diffusion inherent in the former. Comparison of the predictions using both schemes with experiments showed that the second-order upwind scheme produces better agreement (Zurigat and Ghajar, 1990). Recognizing that mixing at the inlet is the major source of stratification degradation and that mixing is inlet-design-dependent, the aim was to find if there exist conditions under which the effect of the inlet geometry on stratification vanishes. Therefore, simulations were conducted for the charging of a hot

water storage tank with two different inlet configurations, each at Richardson numbers ranging from 5.0 to 46.0, where *Ri* was based on the height of the tank and the tank bulk fluid velocity. The first inlet, a *solid-disk diffuser*, consisted of a circular solid disk of diameter 25.4 mm located 12.7 mm from the inlet pipe, which was of the same diameter and located at the center of the top of the tank. The tank had a diameter of 406.0 mm and a height of 1450 mm. The second inlet, the *perforated inlet*, was formed by adding to the *solid-disk diffuser* a perforated extension which spanned the rest of the tank's cross-sectional area. The Richardson number was modified by varying the temperature difference between the inlet and the initial water while maintaining the same flow rate. Figure 6.19 shows the predictions of thermocline in the storage tank as the thermocline passes through different levels close to the inlet region. The temperature profiles shown were obtained by averaging the temperature field at each horizontal level. It is seen that the addition of the perforated extension to the solid-disk diffuser has resulted in a varying degree of improvement in stratification level in the tank depending on the Richardson number.

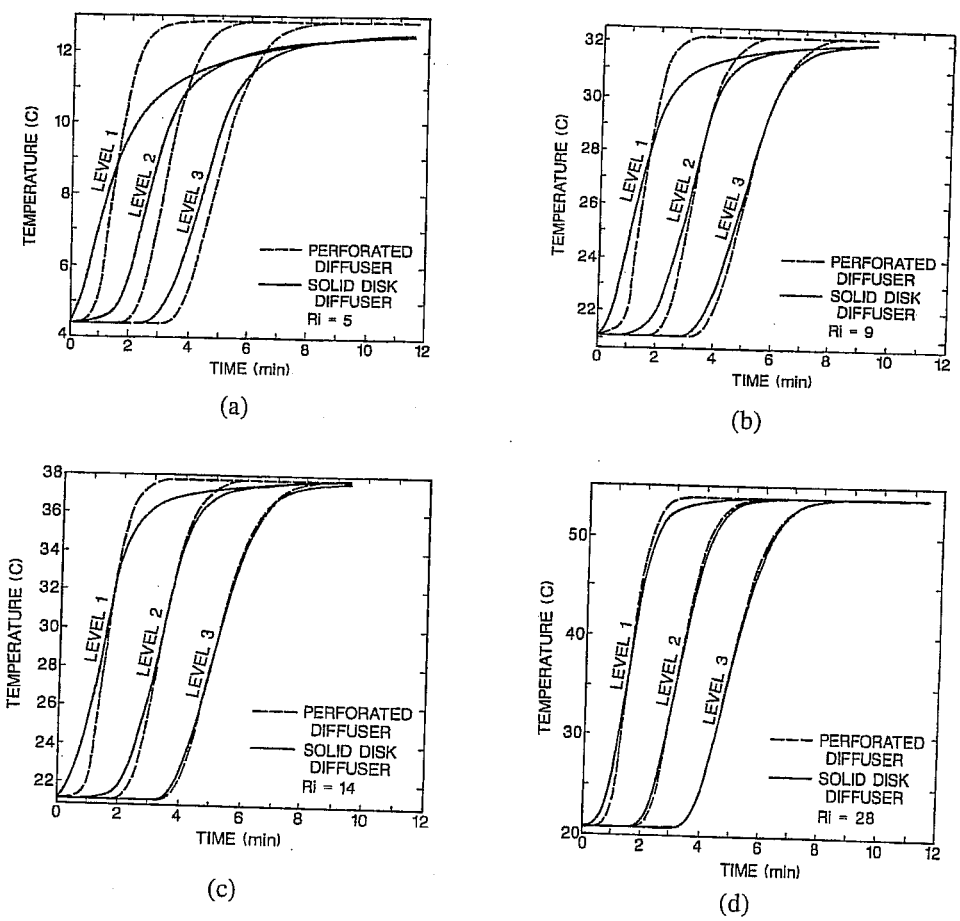

Figure 6.19 Predicted transient temperature profiles at different levels in the tank at different values of Richardson number for two different inlet configurations (Ghajar and Zurigat, 1991).

Consequently, significant improvement is observed at $Ri = 5$. As Ri increases beyond 9.0 the difference in performance of the two inlets becomes insignificant. It was concluded that in thermocline TES tanks, the inlet geometry has a significant effect on stratification for Ri ≤ 5.0 and a negligible effect for $Ri \geq 10$.

Using the same explicit numerical algorithm, i.e. the SOLA algorithm of Hirt *et al.* (1975), Mo and Miyatake (1996) solved the conservation equations in cartesian coordinates to study the charging of the storage tank with hot water. The inlet and outlet ports were of side slot form, located on the upper and lower corners, respectively, on opposite sides. This study included two new elements in stratified thermal storage work: the use of the QUECKEST discretization scheme of Leonard (1979) which is third-order accurate in both space and time to solve the energy equation and the use of the k-ε turbulence model. Again, comparison with the experimental data showed that the first-order upstream difference scheme produces large numerical diffusion while the QUECKEST scheme produces better agreement with the experiments. The results for different values of the Richardson number ranging from 0.005 to 1.545 at a fixed Reynolds number of 500 show that thermal stratification is maintained at Richardson numbers as low as 0.093. The Reynolds and Grashof numbers, and hence the Richardson number, were based on the slot width and the average velocity at the inlet slot. Mo and Miyatake (1996) concluded that at high Richardson numbers the one-dimensional plug-flow model is justified. At $Ri = 0.005$ severe mixing and short-circuiting of the hot fluid directly to the outlet occurs.

To this end the finite-volume numerical method had not been used in the predictions of flow and heat transfer in stratified thermal storage tanks. Lightstone *et al.* (1989) were probably the first to use this method to solve the stratified thermal storage tank problem. The conservation equations in primitive variables and in axisymmetric cylindrical coordinates were solved. Heat conduction in the tank wall was also included to investigate the effect of wall thermal conductivity. Simulations of tank charging with hot water were carried out for both laminar and turbulent flows. The buoyant jet turbulence model described below in this section was used. Lightstone *et al.* (1989) simulated the experiments of Loehrke and Holzer (1979) in which two different inlet configurations were used: the cup diffuser (see Figure 6.3) and a vertical pipe inlet. Good agreement with the experiments with the cup diffuser was achieved using laminar flow calculations, whereas for the vertical pipe inlet the buoyant jet turbulence model was necessary to achieve good agreement. The results showed that for the vertical pipe inlet the two-dimensional nature of the flow was quite obvious by the large radial temperature variation. For both inlets, mixing and two-dimensional flow behavior were observed to occur, at the early stages of charge, on the tail side of the thermocline while one-dimensional flow behavior dominated the rest of the tank. This is in accord with most experimental results.

Stewart *et al.* (1992) investigated the downward impingement of a cold stream from a slot onto the bottom of a chilled water storage tank filled with warmer water and with no bounding walls. The governing steady two-dimensional flow and energy equations expressed in stream function-vorticity formulation along with the turbulence kinetic energy and length scale (k-ℓ) turbulence model equations were solved by finite difference methods. The flow and geometric parameters investigated were the slot width, W, the distance from the jet exit to the tank bottom, h, the Reynolds number based on jet exit mean velocity, and the difference between the cold and warm water temperatures. Adiabatic boundary conditions were assumed and the initial transients were neglected. The isotherms obtained for different parameters indicated that the temperature difference did not influence

the stratification and the other parameters, i.e. Reynolds number, the ratio h/W and W have the dominant effects. Thermal stratification was observed to occur for 50 m < ReW < 200 m at a fixed W/h of unity with W varying between 0.05 and 0.2 m. The steadiness assumed and the absence of side walls are two restrictions that may limit the validity of the results.

In their investigation of the charging of a chilled water storage tank, Cai *et al.* (1993) solved the governing equations in vorticity-stream function formulation and in cartesian coordinates for the turbulent flow case using the k-ℓ turbulence model. An explicit finite-difference method was employed with upwind difference scheme used for the convective terms. The inlet port used was a side slot located at the lower part of the side wall. The results showed that stratification was good at Richardson numbers greater than 5 provided the Reynolds number is less than 10,000 where both are based on the width of the slot and the average velocity at the inlet slot. Doubling the width of the tank while keeping other variables fixed resulted in a thicker thermocline and larger nonuniformity in the horizontal temperature distribution.

Hahne and Chen (1998) studied the charging of a cylindrical hot water storage by solving the laminar flow equations using the vorticity-stream function formulation. The flow inlet and exit were located at the top and bottom of the tank on the centerline. The effects of different storage tank parameters on stratification were studied in terms of the charging efficiency (see Equation 6.10). It was found that for Ri > 0.25 the charging efficiency is essentially unaffected by the increase in Peclet number, where both numbers are based on the inlet velocity and the height of the tank. One-dimensional flow behavior was observed at Ri > 2.5. Computations were also conducted by Spall (1998) for the charging of a cylindrical chilled water storage tank with a peripheral side slot inlet. The turbulent flow and energy equations were solved using two different turbulence models, the k-ε and the Reynolds Stress Model (RSM). A commercial computer program based on the finite-volume method was used and fairly fine-grid solutions were obtained for different Reynolds and Richardson numbers. The results demonstrated that at fixed values of the Richardson number stratification is independent of the Reynolds number, and for good stratification the Richardson number should be greater than 2. Also, Spall (1998) found that the k-ε model predicted a 50–100% thicker thermocline compared with the RSM predictions. Thus, the k-ε model is more diffusive and the predictions using the RSM model are more accurate. The dependence of stratification on the Richardson number alone arrived at in this study is in accord with that of Mo and Miyatake (1996). However, the experimental data of Wildin (1990) for different diffusers with the same inlet Froude number has revealed that the inlet Reynolds number has a strong influence on thermocline development. This is an issue that needs further study.

Based on the studies presented in this section it is evident that the Richardson number is an important parameter that governs the flow and stratification in stratified thermal storages. The design of stratified TES tanks should be based on maximizing this number within reasonable trade-offs. In heating applications this is easily achieved in view of the high buoyancy differentials available. It was demonstrated that there exists an upper limit on the Richardson number beyond which all current inlet designs in thermocline thermal storage perform equally well. In chilled water storage it is more difficult to achieve high Richardson numbers. In this case, the diffuser design is critical for maintaining stratification. Well designed inlets for chilled water storage are those which introduce the flow at a low velocity in a gravity and surface currents for the charge and discharge modes, respectively.

For the sake of completeness, two simple turbulence models are presented below. These are the *Eddy Viscosity* and the *Vertical Buoyant Jet* turbulence models. In the *Eddy Viscosity* model (Sha *et al.*, 1980) the turbulence viscosity is given by

$$\mu_t = 0.007\, C_\mu \rho U_{\max} \ell \tag{6.43}$$

where $U_{max} = max(u, v)$, $\ell = max(\Delta x, \Delta y)$, and C_μ is a constant given by:

$$C_\mu = \begin{cases} 0.1 & \text{for} \quad \mathrm{Re}_{\max} > 2000 \\ 0.1(0.001\,\mathrm{Re}_{\max} - 1) & \text{for} \quad 1000 \le \mathrm{Re}_{\max} \le 2000 \\ 0 & \text{for} \quad \mathrm{Re}_{\max} < 1000 \end{cases} \tag{6.44}$$

Also, $Re_{max} = max(Re_x, Re_y)$, where $Re_x = \rho u \Delta y/\mu$, $Re_y = \rho v \Delta x/\mu$. The turbulence conductivity is calculated from:

$$k_t = \frac{C_p \mu_t}{\mathrm{Pr}_t} \tag{6.45}$$

where the turbulent Prandtl number Pr_t is evaluated as

$$\mathrm{Pr}_t = 0.8[1 - \exp(-6x10^{-5}\,\mathrm{Re}_{\max}\,\mathrm{Pr}^{1/3})]^{-1} \tag{6.46}$$

In the *Vertical Buoyant Jet* turbulence model (Lightstone *et al.*, 1989) the flow field in the storage tank is divided into three regions, taking into account the nature of the forces acting on the jet issuing from the inlet port and the bulk fluid motion in the tank. These three regions are:

1. The *jet region*: flow here is momentum driven. Axially, this region extends from the inlet port to a distance at which the jet centerline velocity reaches 10% of its initial value. Radially, the jet region extends from the jet centerline to a distance where the jet velocity changes sign. The turbulence viscosity is calculated using the standard jet model:

$$\mu_t = c\rho\, bv \tag{6.47}$$

   where b and v at the given elevation are the jet half width and the centerline velocity, respectively, and c is a constant (0.0256). Clearly, μ_t does not vary radially if the density remains constant.
2. The *plume region*: the flow in this region is gravity driven in the direction opposite to the jet flow. The plume region extends radially from the outer boundary of the jet region to the locations where the buoyant flow changes direction. In this region the turbulence viscosity is calculated using the same relation given above with $c = 0.068$.
3. The *rest-of-the-tank region:* the flow is unidirectional and constitutes the bulk fluid motion towards the outlet. In this region the flow is assumed laminar.

It must be noted that the boundaries between these regions change with time, and thus should be updated along with μ_t after each time step.

6.7 Conclusions

Stratified thermal energy storage for hot or chilled water fluids has become a common tool in energy conservation and management technology. In this chapter the theoretical and experimental foundations of stratified TES were reviewed. The fluid flow and heat transfer aspects of the subject were introduced and performance measures used by different investigators presented. Design parameters governing the performance of stratified TES were identified. In general, for stratified tanks to perform as expected, several design recommendations must be kept in mind. First, the inlet temperature should be maintained constant whenever possible. Mixing is greatly enhanced by inflows having a variable inlet temperature. The requirement of constant inlet temperature is not difficult to satisfy in chilled water storage systems. However, these systems operate under small density differentials, and thus the inlet diffuser design is critical for maintaining stratification. In solar energy storage applications a variable inlet temperature is more common, and thus maintaining stratification under this condition is difficult. Practical distributors that direct the incoming flow to its temperature level with minimal mixing are not yet reliable. Moreover, they are not flexible in design. More work in this area is still needed. Alternatively, as proposed by some researchers, the solar energy collection strategy may need to be altered to maintain a nearly constant inlet temperature. In thermocline TES tanks the inflow must be introduced at the uppermost and the lowermost levels in the tank for the charging of hot and chilled water storage tanks, respectively. The reverse is true for discharging. Furthermore, the inlet velocity must be maintained at a minimum by using inlet diffusers. In this regard, the diffusers developed for chilled water storage are generally recommended as they will perform even better in hot water storage tanks because of the higher buoyancy differential under which these tanks operate. In thermocline hot water storage there exist flow conditions under which the inlet geometry has a negligible effect on stratification. These conditions are characterized by Ri greater than 10 where the Ri is based on the height of the tank and the water bulk velocity in the tank.

Further recommendations relate to the tank aspect ratio which should be maintained between 3 and 4, and the tank material which should be made of material having a thermal conductivity as close as possible to that of water. This may also be achieved by insulating the interior of the storage tank. This recommendation regarding the tank material is important if the tank is to stay idle while partially charged or discharged. The dimensionless numbers characterizing the flow and heat transfer in stratified TES tanks represent reliable guides for design. However, these numbers should be interpreted in view of the reference velocity and length scales used.

The importance of one-dimensional flow models lies in the fact that they are computationally more efficient than two- or three-dimensional models, which makes them ideal for incorporation into overall energy-system simulation programs. Furthermore, one-dimensional flow should be the target of stratified TES tank designs in practice, as two- or three-dimensional flow would only enhance mixing and degrade the performance. Two- and three-dimensional models, on the other hand, are more capable in accounting for a broad range of hydrodynamic, thermal, and geometric conditions. These models can be used for design assessments and testing of innovative design concepts. The literature on stratified thermal storage is still lacking in the area of three-dimensional modeling. This is understandable in view of the complexity and computational cost involved.

Acknowledgements

We are indebted to the University Center for Energy Research at Oklahoma State University for providing the funding for most of this work. We are also indebted to Ms. Diane Compton for her superb help with the manuscript.

Nomenclature

A	Area
C	Courant number ($C = V\Delta t / \Delta x$)
C_p	specific heat at constant pressure
Ex	exergy
f	friction factor
Fo	Fourier number ($Fo = \alpha\Delta t / (\Delta x)^2$)
Fr	Froude number ($Fr = u_r / \sqrt{g\ell_r}$)
Fr_m	modified Froude number ($Fr_m = u_r / \sqrt{g\beta(T - T_r)\ell_r}$)
Fr_{dm}	densimetric modified Froude number ($Fr_{dm} = u_r / \sqrt{g\ \ell_r(\rho_r - \rho)/\rho_r}$)
g	acceleration of gravity
Gr	Grashof number ($Gr = g\beta(T - T_r)\ell_r^3 / \nu^2$)
h	enthalpy in Equation 6.16 and height elsewhere
H	effective height between tank inlet and outlet
k	thermal conductivity
L	length (also the tank height in the ratio X/L when used in the figures)
l	length scales associated with the resistance terms in Equations 6.38 and 6.39
ℓ	turbulence length scale
ℓ_r	reference length
M	mass (or moment in Equations 6.14 and 6.15
$\dot{m}$	mass flow rate
p	pressure
P	perimeter
Pr	Prandtl number ($Pr = \mu C_p / k$)
Pe	Peclet number ($Pe = u_r \ell_r / \alpha$)
q	heat transfer rate
Q	heat transfer
r	radius
Re	Reynolds number ($Re = \rho u_r \ell_r / \mu$)
R_x, R_y	resistance force components in the x and y directions defined by Equations 6.38 and 6.39
Ri	Richardson number ($Ri = g\beta\Delta T \ell_r / u_r^2$)
Ri_d	densimetric Richardson number ($Ri_d = g(\rho - \rho_r)\ell_r / \rho_r u_r^2$)
s	entropy

S heat loss parameter ($S = UPH^2/A_c k$)
t time
t^* dimensionless time ($t^* = V t/H$)
T temperature
T^* dimensionless temperature ($T^* = (T - T_o)/(T_{in} - T_o)$)
u velocity in the x- or r-direction
u_r reference velocity
v velocity in the y-direction
V average vertical velocity in the tank
U overall heat transfer coefficient
x Cartesian or cylindrical ($x = r$) coordinate in Equations 6.37–6.40 and distance from the inlet in Figure 6.8 and Equations 6.22–6.28
X distance from the inlet
y vertical coordinate

Greek Symbols

α thermal diffusivity
β coefficient of thermal expansion [$\beta = (\rho_r - \rho)/(\rho_r (T - T_r))$]
ε turbulence energy dissipation rate
ε_H Eddy diffusivity for heat
η efficiency
Δ designates difference when used as prefix
μ dynamic viscosity
ν kinematic viscosity
ρ density
ξ index for Cartesian ($\xi = 0$) or cylindrical ($\xi = 1$) coordinates

Special Symbols

$\forall$ volume
$\dot{\forall}$ volume flow rate

Subscripts

a ambient
c charge (or cross section when with area A)
d discharge
E energy
e exit
eff effective
h high
in inlet
ℓ low (when with T) and laminar (with μ or k)
m mass

r	reference
t	turbulence
th	thermal
T	tank (or total)
o	initial

Superscripts

in	inlet
*	dimensionless quantity

References

Abdoly, M.A. (1981). *Thermal Stratification in Storage Tanks*, PhD Thesis, University of Texas at Dallas.

Abdoly, M.A. and Rapp, D. (1982). Theoretical and experimental studies of stratified thermocline storage of hot water, *Energy Conversion and Management* 22, 275–285.

Abu-Hamdan, M.G., Zurigat, Y.H. and Ghajar, A.J. (1992). An experimental study of a stratified thermal storage under variable inlet temperature for different inlet designs, *International Journal Heat and Mass Transfer* 35, 1927–1934.

Al-Marafie, A., Al-Kandari, A. and Ghaddar, N. (1991). Diffuser design influence on the performance of solar thermal storage tanks, *International Journal of Energy Research* 15, 525–534.

Al-Najem, N.M. (1993). Degradation of a stratified thermocline in a solar storage tank, *International Journal of Energy Research* 17, 183–191.

Al-Najem, N.M., Al-Marafie, A. and Ezuddin, K.Y.(1993). Analytical and experimental investigation of thermal stratification in storage tanks, *International Journal of Energy Research* 17, 77–88.

Al-Najem, N.M. and El-Refaee, M.M. (1997). Numerical study of the prediction of turbulent mixing factor in thermal storage tanks, *Applied Thermal Engineering* 17, 1173–1181.

Baines, W.D., Martin, W.W. and Sinclair, L.A. (1982). On the design of stratified thermal storage tanks, *ASHRAE Transactions* 88, 426–439.

Brumleve, T.D. (1974). *Sensible Heat Storage in Liquids*, Sandia Labs Report, SLL-73-0263.

Cabelli, A. (1977). Storage tanks-A numerical experiment, *Solar Energy* 19, 45–54.

Cai, L., Stewart, W.E. and Sohn, C.W. (1993). Turbulent buoyant flows into a two dimensional storage tank, *International Journal Heat and Mass Transfer* 36, 4247–4256.

Chan, A.M.C., Smereka, P.S. and Guisti, D. (1983). A numerical study of transient mixed convection flows in a thermal storage tank, *ASME-Journal Heat Transfer* 105, 246–253.

Close, D.J. (1967). A design approach for solar processes, *Solar Energy* 11, 112–122.

Cole, R.L. and Bellinger, F.O. (1982). Thermally stratified tanks, *ASHRAE Transactions* 88, Part 2(1), 1005–1017.

Davidson, J.H. and Adams, D.A. (1994). Fabric stratification manifolds for solar water-heating, *Journal of Solar Energy Engineering* 116, 130–136.

Davidson, J.H., Adams, D.A. and Miller, J.A. (1994). A coefficient to characterize mixing in solar water storage tanks, *Journal of Solar Energy Engineering* 116, 94–99.

Davis, E.S. and Bartera, R. (1975). Stratification in solar water heater storage tank, *Proceedings of the Workshop on Solar Energy Storage Subsystems for the Heating and Cooling of Buildings*, Charlottesville, Virginia, pp. 38–42.

Duffie, J.A. and Beckman, W.A. (1980). *Solar Engineering of Thermal Processes*, Wiley, New York.

Gari, H.N., Loehrke, R.I. and Holzer, J.C. (1979). Performance of an inlet manifold for a stratified storage tank, *ASME Paper 79-HT-67, Joint ASME/AICHE 18th National Heat Transfer Conference*, San Diego, California, August.

Ghajar, A.J. and Zurigat, Y.H. (1991). Numerical study of the effect of inlet geometry on mixing in thermocline thermal energy storage, *Numerical Heat Transfer*-Part A 19, 65–83.

Gretarsson, S.P., Pedersen, C.O. and Strand, R.K. (1994), Development of a fundamentally based stratified thermal storage tank model for energy analysis calculations, *ASHRAE Transactions* 100, 1213–1220.

Gross, R.J. (1982), An experimental study of single medium thermocline thermal energy storage, *ASME Paper 82-HT-53*.

Guo, K.L. and Wu, S.T. (1985). Numerical study of flow and temperature stratification in a liquid storage tank, *Journal of Solar Energy Engineering* 107, 15–20.

Hahne, E. and Chen, Y. (1998), Numerical study of flow and heat transfer characteristics in hot-water stores, *Solar Energy* 64, 9–18.

Han, S.M. and Wu, S.T. (1978). Computer simulation of a solar energy system with a viscous-entrainment liquid storage tank model, *Proceedings of the Third Southeastern Conference on Application of Solar Energy*, Edited by Wu, S.T., Christensen, D.L. and Head, R.R., 165–182

Han, S.M. and Wu, S.T. (1985). Enhancement of thermal stratification in a liquid storage tank by a horizontal baffle, In: *Fundamentals of Forced and Mixed Convection*, a collection of papers presented at the 23d National Heat Transfer Conference, Denver, Colorado (Edited by F.A. Kulacki and R.D. Boyd), pp. 197–205.

Hess, C.F. and Miller, C.W. (1982). An experimental and numerical study on the effect of the wall in a cylindrical enclosure-I, *Solar Energy* 28, 145–152.

Hirt, C.W., Nichols, B.D. and Romero, N.C. (1975). *SOLA: A Numerical Solution Algorithm for Transient Fluid Flows*, Report LA-5852, Los Alamos Scientific Laboratory, New Mexico.

Hollands, K.G.T. and Lightstone, M.F. (1989). A review of low-flow, stratified tank solar water heating systems, *Solar Energy* 43, 97–106.

Homan, K.O., Sohn, C.W. and Soo, S.L. (1996). Thermal performance of stratified chilled water storage tanks, *HVAC & R Research* 2, 158–170.

Ismail, K.A.R., Leal, J.F.B. and Zanardi, M.A. (1997). Models of liquid storage tanks, *International Journal of Energy Research* 22, 805–815.

Jaluria, Y. and Gupta, S.K. (1982), Decay of thermal stratification in water body for solar energy storage, *Solar Energy* 28, 137–143.

Kleinback, E.M., Beckman, W.A. and Klein, S.A. (1993). Performance study of one-dimensional models for stratified thermal storage tanks, *Solar Energy* 50, 155–166.

Kuhn, J.K., von Fuchs, G.F. and Zob, A.P. (1980). *Developing and Upgrading of Solar-System Thermal-Energy-Storage Simulation Models*, Final Report, prepared by Boeing Computer Services Company for the Department of Energy, Contract DE-AC02-77CS 34482.

Lavan, Z. and Thompson, J. (1977). Experimental study of thermally stratifed hot water storage tanks, *Solar Energy* 19, 519–524.

Leonard, B.P.(1979). Stable and accurate convective modeling procedure based on quadratic upstream interpolation, *Computational Methods in Applied Mechanical Engineering* 19, 59–98.

Lightstone, M.F., Raithby, G.D. and Hollands, K.G.T. (1989). Numerical simulation of the charging of liquid storage tanks: Comparison with experiment, *Journal of Solar Energy Engineering* 111, 225–231.

Loehrke, R.I., Gari, H.N. and Holzer, J.C. (1979). *Thermal Stratification Enhancement for Solar Energy Applications*, Technical Report HT-TS792, Prepared for the Civil Engineering Laboratory, Naval Construction Battalion Center, Port Hueneme, California.

Loehrke, R.I. and Holzer, J.C. (1979). *Stratified Thermal Storage Experiments*, Technical Report HT-TS793, Mechanical Engineering Department, Colorado State University, Fort Collins, Colorado.

Mavros, P., Belessiotis, V. and Haralambopoulos, D. (1994). Stratified energy storage vessels-characterization of performance and modeling of mixing behaviour, *Solar Energy* 52, 327–336.

Miller, C.W. (1977). Effect of conducting wall on a stratified fluid in a cylinder, *AIAA Paper No. 77-792, AIAA 12th Thermophysics Conference*, Albuquerque, New Mexico.

Mo, Y. and Miyatake, O. (1996). Numerical analysis of the transient turbulent flow field in a thermally stratified thermal storage tank, *Numerical Heat Transfer*-Part A 30, 649–667.

Musser, A. and Bahnfleth, W.P. (1998). Evolution of temperature distribution in a full-scale stratified chilled-water storage tank with radial diffusers, *ASHRAE Transactions* 104, Part 1A, 55–67.

Murthy, S.S., Nelson, J.E.B. and Rao, T.L.S. (1992). Effect of wall conductivity on thermal stratification, *Solar Energy* 49, 273–277.

Nakahara, N., Sagara, K. and Tsujimoto, M. (1988). Water thermal storage tank: Part 2-mixing model and storage model estimation for temperature stratified tanks, *ASHRAE Transactions* 94, Part 2, 371–394.

Nelson, J.E.B., Balakrishnan, A.R. and Murthy, S.S. (1999). Experiments on stratified chilled water tanks, *International Journal of Refrigeration* 22, 216–234.

Oppel, F.J., Ghajar, A.J. and Moretti, P.M. (1986). A numerical and experimental study of stratified thermal storage, *ASHRAE Transactions* 92, 293–309.

Patankar, S.V. (1980). *Numerical Heat Transfer and Fluid Flow*, McGraw-Hill.

Philips, W.F. and Dave, R.N. (1982). Effect of stratification on the performance of liquid-based solar heating systems, *Solar Energy* 29, 111–120.

Rosen, M.A. (1991). On the importance of temperature in performance evaluations for sensible thermal energy storage systems, *Proceedings of the Biennial Congress of the International Solar Energy Society*, Denver, Colorado, USA, 19–23 August. In 1991 Solar World Congress, vol. 2, Part. II (Eds: Arden, M.E., Burley, S.M.A. and Coleman, M.), pp.1931–1935.

Rosen, M.A. and Hooper, F.C. (1991). Evaluation of energy and exergy contents of stratified thermal energy storages for selected storage-fluid temperature distributions, *Proceedings of the Biennial Congress of the International Solar Energy Society*, Denver, Colorado, USA, 19–23 August. In 1991 Solar World Congress, vol. 2, Part. II (Eds: Arden, M.E., Burley, S.M.A. and Coleman, M.), pp. 1961–1966.

Sha, W.T. and Lin, E.I.H. (1978). Three dimensional mathematical model of flow stratification in thermocline storage tanks, In: *Application of Solar Energy* (Edited by S.T. Wu *et al.*), pp.185–202.

Sha, W.T., Lin, E.I.H. Schmitt, R.C., Lin, K.V., Hull, J.R., Oras, J.J. and Domanus, H.M. (1980). *COMMIX-SA-1: A Three-Dimensional Thermodynamic Computer Program for Solar Applications*, Argonne National Laboratory Report, ANL-80-8.

Sharp, M.K. (1978). *Thermal Stratification in Liquid Sensible Heat Storage*, MSc Thesis, Colorado State University, Fort Collins, Colorado.

Sharp, M.K. and Loehrke, R.I. (1979). Stratified thermal storage in residential solar energy applications, *Energy* 3, 106–113.

Sliwinski, B.J., Mech, A.R. and Shih, T.S. (1978). Stratification in thermal storage during charging, *Proceedings of the 6th International Heat Transfer Conference*, Toronto, vol. 4, pp. 149–154.

Spall, R.E. (1998). A numerical study of transient mixed convection in cylindrical thermal storage tanks, *International Journal of Heat and Mass Transfer* 41, 2003–2011.

Stewart Jr., W.E., Becker, B.R., Cai, L. and Sohn, C.W. (1992). Downward impinging flows for stratified chilled water storage, *Proceedings of the 1992 ASME National Heat Transfer Conference,* HTD-vol. 206-2, pp. 131–138.

Tamblyn, R.T. (1980). Thermal storage resisting temperature blending, *ASHRAE Journal* 22, 65–70.

Tran, N., Kreider, J.F. and Brothers, P. (1989). Field measurement of chilled water storage system thermal performance, *ASHRAE Transactions* 95, Part 1, 1106–1112.

Van Koppen, C.W.J., Thomas, J.P.S. and Veltcamp, W.B. (1979). The actual benefits of thermally stratified storage in small and medium size solar system, *Proceedings of ISES Biennial Meeting,* Atlanta, GA, Pergamon Press, New York, vol. 2, pp. 576–580.

Votsis, P.P., Tasson, S.A., Wilson, D.R. and Marquand, C.J. (1988). Experimental and theoretical investigation of mixed and stratified hot water storage tanks, *Proceedings of the Institution of Mechanical Engineers, Part C-Journal of Mechanical Engineering Science* 202, 187–193.

Wuestling, M.D., Klein, S.A. and Duffie, J.A. (1985). Promising control alternatives for solar water heating systems, *Journal of Solar Energy Engineering* 107, 215–221.

Wildin, M.W. (1989). Performance of stratified vertical cylindrical thermal storage tanks, Part II: Prototype tank, *ASHRAE Transactions* 95, Part 1, 1096–1105.

Wildin, M.W. (1990). Diffuser design for naturally stratified thermal storage, *ASHRAE Transactions* 96, Part 1, 1094–1102.

Wildin, M.W. (1991). Flow near the inlet and design parameters for stratified chilled water storage, *National Heat Transfer Conference,* Minneapolis, MN, July 28–31.

Wildin, M.W. (1996). Experimental results from single-pipe diffusers for stratified thermal energy storage, *ASHRAE Transactions* 102, Part 2, 123–132.

Wildin, M.W. and Sohn, C.W. (1993). *Flow and Temperature Distribution in a Naturally Stratified Thermal Storage Tank,* USACERL Technical Report FE-94/01.

Wildin, M.W. and Truman, C.R. (1985a). A summary of experience with stratified chilled water tanks, *ASHRAE Transactions* 92, 956–976.

Wildin, M.W. and Truman, C.R. (1985b). *Evaluation of Stratified Chilled Water Storage Technique,* EPRI Report, EPRI EM-4352, December.

Wildin, M.W. and Truman, C.R. (1989). Performance of stratified vertical cylindrical thermal storage tanks, Part I: Scale model tank, *ASHRAE Transactions* 95, Part 1, 1086–1095.

Wyman, C., Castle, J. and Kreith, F. (1980). A review of collector and energy storage technology for intermediate temperature applications, *Solar Energy* 24, 517–540.

Yoo, J., Wildin, M.W. and Truman, C.R. (1986). Initial formation of a thermocline in stratified thermal storage tanks, *ASHRAE Transactions* 92, Part 2A, 280–291.

Zurigat, Y.H. (1988). *An Experimental and Analytical Examination of Stratified Thermal Storage,* PhD Thesis, Oklahoma State University, Stillwater, Oklahoma, December.

Zurigat, Y.H., Ghajar, A.J. and Moretti, P.M. (1988). Stratified thermal energy storage tank inlet mixing characterization, *Applied Energy* 30, 99–111.

Zurigat, Y.H., Maloney, K.J. and Ghajar, A.J. (1989). A comparison study of one-dimensional models for stratified thermal storage tanks, *Journal of Solar Energy Engineering* 111, 204–210.

Zurigat, Y.H. and Ghajar, A.J. (1990). A comparative study of weighted upwind and second order difference schemes, *Numerical Heat Transfer*-Part B, 18, 61–80.

Zurigat, Y.H., Liche, P.R. and Ghajar, A.J. (1991). Influence of inlet geometry on mixing in thermocline thermal energy storage, *International Journal of Heat and Mass Transfer* 34, 115–125.